The Role of MCP-1 in Epithelial to Mesenchymal Transition and Invasion during Early Mammary Carcinogenesis

by

Matthew Aaron Thomas Sweede

Department of Pharmacology & Cancer Biology
Duke University

Date:_____

Approved:

_____
Victoria Seewaldt, Supervisor

_____
Ann Marie Pendergast

_____
Jeffrey Rathmell

_____
Mariano Garcia-Blanco

_____
Robin Bachelder

Thesis submitted in partial fulfillment of
the requirements for the degree of
Master of Science in the Department of
Pharmacology & Cancer Biology in the
Graduate School of Duke University

2013

ABSTRACT

The Role of MCP-1 in Epithelial to Mesenchymal Transition and Invasion during Early Mammary Carcinogenesis

by

Matthew Aaron Thomas Sweede

Department of Pharmacology & Cancer Biology
Duke University

Date:_____

Approved:

_____
Victoria Seewaldt, Supervisor

_____
Ann Marie Pendergast

_____
Jeffrey Rathmell

_____
Mariano Garcia-Blanco

_____
Robin Bachelder

An abstract of a thesis submitted in partial
fulfillment of the requirements for the degree
of Master of Science in the Department of
Pharmacology & Cancer Biology in the Graduate School of
Duke University

2013

Abstract

Triple negative breast cancers are aggressive breast tumors that are characterized by the absence of estrogen receptor, progesterone receptor, and HER2. This absence of expression limits targeted therapeutic strategies. The result is a disease that is associated with a poor prognosis. The current survival rate for those afflicted with triple negative breast cancer is 77%. This survival rate is compared to a 93% survival rate for all other breast cancers combined. Furthermore, triple negative breast cancers disproportionately affect young and African American women.

The Carolina Breast Cancer Study demonstrated that obesity increased the risk of triple negative breast cancer in premenopausal women. These findings were supported by a meta-analysis of 11 epidemiological studies evaluating the association between triple negative breast cancer, obesity, and menopause status. Consequently, it is hypothesized that obesity in premenopausal women may contribute to the initiation and progression of triple negative breast cancer.

On average, adipose constitutes 70% of the breast. Obesity is a disease of increased adipose tissue, which can increase the adiposity of the breast. Studies show that obesity enhances the production of the inflammatory cytokines IL1β, IL6, IL8, TNFα, and MCP-1 in adipose tissue. Inflammatory cytokines contribute to proliferation and survival of malignant cells, migration and invasion, and induction of epithelial to mesenchymal transition (EMT).

The purpose of this study is to investigate the role of adipose derived cytokines in promotion of EMT and invasion in early mammary carcinogenesis. To study EMT and invasion in early mammary carcinogenesis, a co-culture was generated using adipose stromal cell (ASC) conditioned media and the non-transformed, mammary epithelial cell line MCF10A. ASC-conditioned media was characterized for cytokine production. Findings indicated that IL6, IL8, and MCP-1 were secreted into the media. Researchers have extensively studied IL6 and IL8 in breast EMT, but the relevance of MCP-1 in breast carcinogenesis has only recently emerged. MCP-1 is involved in monocyte and macrophage trafficking, renal fibrosis and EMT, as well as EMT in peritoneal disease. The role of MCP-1 in renal and peritoneal EMT suggests that MCP-1 may induce EMT in mammary epithelial cells.

MCP-1 did not alter the protein expression levels of either E-cadherin or Vimentin in 2D culture. MCP-1 treatment did, however, rapidly phosphorylate Erk1/2 at T202/Y204 and induce chemotaxis of MCF10A cells in a Boyden Chamber migration assay. Erk1/2 phosphorylation and chemotaxis were inhibited by pretreatment with PD98059, a potent small molecule inhibitor of Erk signaling.

In 3D, MCF10A acini treated with MCP-1 lost expression of E-cadherin, β-catenin, and localized areas of Integrin α6. Additionally, MCP-1 induced outgrowth away from the MCF10A spheroids and invasion into the extracellular matrix during a spheroid gel invasion assay. MCP-1 did not induce the secretion of MMP-2 or MMP-9 during invasion. When the MCP-1 treated acini and spheroids were co-treated with PD98059 E-cadherin loss and invasion were inhibited respectively. This inhibition

suggests that Erk activation is necessary for E-cadherin loss and cell invasion. The data indicate that MCP-1 plays a potential role in the early EMT and invasion of non-transformed, mammary epithelial cells. This study provides a foundation for the study of MCP-1 induced EMT and invasion in MCF10A cells. Further work will need to be completed to elucidate the mechanism by which MCP-1 decreases E-cadherin and induces invasion.

Dedication

For the three most important women in my life: Samantha Welsch, from whom I derive passion; Nan Sweede, from whom I derive strength; y Magda Pesquera Sweede, de quien deriva mi cultura y amor por la familia.

Contents

List of Tables

List of Figures

Acknowledgements

This investigation was made possible by the contributions of several people who have worked in the Seewaldt lab. The technique for the isolation of adipose stromal cells (ASCs) from primary human adipose tissue was brought into the lab by Stephanie Ellison-Zelski PhD. ASC characterization, differentiation, and IL-6 measurement was completed by Adria Suarez. Adria additionally developed the co-culture of MCF10A cells with ASC-conditioned media. Jenny Hsieh developed the treatment protocol of 3D MCF10A acini with MCP-1.

1 Introduction

Breast cancer is the most common cancer among women (1). According to the National Cancer Institute, based on current incidence rates, 12.4% of women born in the United States today will get breast cancer in their lifetime (2). Despite current incidence rates, there has been an increase in breast cancer survival rates over the past few decades. In 1975, the overall survival rate of women diagnosed with breast cancer in the United States did not exceed 75%. Currently, however, this survival rate is now approaching 90% (3). This increase in survival can be attributed to earlier detection, improved treatment, and targeted therapies.

Breast cancer is not a homogenous disease and is characterized by the expression of its cell surface receptors. Breast cancers are subtyped by the expression of three cell surface receptors: estrogen receptor (ER), progesterone receptor (PR), and human epidermal growth factor receptor 2 (Her2). A breast cancer that lacks the expression of these three receptors is a triple-negative breast cancer (TNBC) (4). Triple negative tumors are associated with a poor prognosis because there are no established targeted therapies. The current survival rate of women with TNBCs is 77%, compared to 93% for all other breast cancer patients combined (5).

1.1 Disparities in Breast Cancer

Triple negative breast cancers occur more often in young and African American women (5-7, 85, 95-99). A study stratifying the age of women diagnosed with TNBC showed that 63.1% of female patients with a triple negative tumor were under the age of 60 (95). The Carolina Beast Cancer Study stratified their patients by menopausal status

and showed that 64% of triple negative tumors occurred in premenopausal women (7). In addition to increased incidences of TNBC, it was shown that young women (31-40 years old) diagnosed with TNBC had a shorter disease-free state and overall length of survival when compared to older women (>60 years old) (96).

African American women are up to three times as likely to be diagnosed with triple negative tumors as Caucasian women (7, 97, 99-100). Additionally, African American women with TNBC have a higher mortality rate than Caucasian women even after adjusting for age, stage, and grade of tumor (97-100).

Within the population of African American women, investigations have shown that young African American women have higher TNBC rates than older African American women. The Carolina Breast Cancer Study showed that TNBC was more prevalent among premenopausal African American women (39%) compared with postmenopausal women (14%). It was further shown that TNBC was less prevalent in non-African American women of any age (16%) (7).

The Carolina Breast Cancer Study then examined the role of obesity in breast cancer subtypes. It was shown that obesity in premenopausal women was associated with increased risk of TNBCs, while obesity in postmenopausal women was associated with increased risk of ER+ breast cancers (9). A meta-analysis of 11 epidemiological studies evaluating the association between TNBC, obesity, and menopause status further supported the findings that obesity was associated with increased risk of TNBC in premenopausal women (101). Consequently, obesity in premenopausal women may contribute to the formation of TNBC.

1.2 Signaling Pathways in TNBC

To better understand the molecular pathways involved in TNBC and identify molecular based therapies, a meta-analysis of 587 triple negative breast tumor gene expression arrays was performed. The investigators identified six distinct molecular subtypes of TNBC (11). Two of these subtypes occur at a higher frequency in African American women and have a worse prognosis: the Mesenchymal-like and Mesenchymal Stem-like. Both subtypes were so named because they were enriched for epithelial-mesenchymal transition (EMT) markers and growth factor pathways. Upon closer observation of the gene set enrichment analysis, it is apparent that the Mesenchymal Stem-like subtype has increased expression of transcripts from genes sets for both adipocytokine signaling pathways (KEGG_Adipocytokine_signaling_pathway - 69 genes) and ERK1/2 signaling pathways (Biocarta_ERK_pathway – 28 genes) (11). Activation of adipocytokine pathways suggests increased adipose signaling, which is associated with obesity (13-15).

Increased Erk1/2 signaling is associated with more aggressive TNBC cases with poorer outcomes. Triple negative breast tumors were measured by reverse phase protein microarray and showed increased phosphorylation of Erk1/2 T202/Y204 and downstream targets (12).

Activation of Erk is associated with obesity. Obesity increases the amount of circulating cytokines produced by adipose tissue (13, 15). Several of these cytokines; IL6, IL8, Leptin, and MCP-1; have been shown to phosphorylate Erk1/2 at T202/Y204 (57-58,

80-82). The increase of circulating cytokines that result in Erk1/2 phosphorylation suggests that obesity correlates with increased Erk signaling in tissues.

Previously published work suggests a link between high-risk TNBC, EMT, and obesity in early mammary carcinogenesis (16). Cytological samples were acquired from a cohort of women who were high risk for breast cancer and analyzed using reverse-phase protein microarray. Women were considered high risk if they had one of the following major risk factors: a 5-year Gail risk calculation of greater than 1.7%; a prior biopsy exhibiting atypical hyperplasia, lobular carcinoma *in situ*, or ductal carcinoma *in situ;* or known BRCA1/2 mutation carrier. It was observed that the mesenchymal marker Vimentin correlated with obesity (16).

Within the same study, it was shown that many of the samples had an increase in Erk1/2 phosphorylation (16). Furthermore, a separate study showed that constitutively activated Erk signaling induced EMT (61).

Taken together, Erk signaling is activated in aggressive TNBC and in early precancerous cytological samples from a cohort of women who are high-risk for breast cancer. Additionally, the mesenchymal marker Vimentin correlated with obesity in the same cohort of women. Lastly, Erk signaling is associated with obesity and has been shown to induce EMT.

1.3 Epithelial-Mesenchymal Transition

Epithelial-mesenchymal transition is defined as a biologic process that allows a polarized epithelial cell, which normally interacts with a basement membrane via its basal surface, to undergo multiple biochemical changes that enable it to assume a

mesenchymal cell phenotype (20). EMT enhances migratory capacity, invasiveness, elevated resistance to apoptosis, and greatly increased production of extracellular matrix (ECM) components (20). Typical of many cancerous processes, the transition from an epithelial state to a mesenchymal state occurs normally during development, but is hijacked by transformed cells (22). EMT is measured by the loss of epithelial markers such as E-cadherin, Cytokeratin, and ZO-1, and by the acquisition of mesenchymal markers such as Vimentin, N-cadherin, and Fribronectin. EMT is controlled by a set of master EMT regulating transcription factors including but not limited to: Twist1/2, Zeb1/2, Snail and Slug (20-23). Furthermore, EMT is commonly associated with TNBC (11, 24) and several triple negative cell lines have been shown to express multiple EMT markers (25).

Both cytokines and growth factors have been shown to induce EMT in a number of transformed and non-transformed cell lines (26-29). The cytokines TGF-β, TNFα, IL6, IL8, and Leptin have all demonstrated induction of EMT *in vitro* (26-30, 32-33, 89). Most of these cytokines are also secreted by adipose tissue, which makes up an average of 70% of the breast microenvironment (13, 34).

1.4 Breast Microenvironment

The breast terminal ductal lobular unit is composed of a layer of luminal epithelial cells surrounded by myoepithelial cells, which are attached to a basement membrane. Encompassing the terminal ductal lobular unit are stromal cells, which include endothelial and immune cells, fibroblasts and adipocytes. Extracellular matrix proteins secreted by stromal cells support the branching duct structure. Additionally,

cytokines are secreted by all of the cells surrounding the terminal ductal lobular unit (35). Subcutaneous adipose tissue surrounds the branching ducts and terminal ductal lobular units (34-35).

1.4.1 Adipose Tissue

Adipose tissue was once viewed as an inert tissue that provided insulation to the body. Now, adipose tissue is recognized as an endocrine organ that secretes hormones, cytokines, chemokines, growth factors and adipokines (36). On average, the breast is composed of 70% adipose tissue (34). Obesity increases the inflammatory cytokines IL1β, IL6, IL8, TNFα, and MCP-1 in adipose tissue (35-37, 50-51, 81, 87-88). Recognizing this, several groups have studied the cytokines and growth factors secreted by adipose tissue in *in vitro* transformed cell and non-transformed cell models (37-39). While not exhaustive, this list includes: IL6, IL8, IL1β, TNFα, VEGF, HGF, M-CSF, leptin and adiponectin (13, 39).

1.4.1.1 Adipose in Cell Culture

Mature adipocytes are terminally differentiated, and thus, will not grow in culture. Therefore, *in vitro* studies are difficult to perform. To overcome this obstacle, researchers have devised different approaches to studying adipose cytokine production on different cell lines. The crudest way to study this is to incubate adipose tissue collected from a patient directly in media, and to collect the media for use on cell lines (40). This method uses primary mature adipocytes, but included in the adipose tissue are other stromal cells: fibroblasts and immune cells. Additionally, it is not possible to control cell numbers when using primary patient adipose tissue to condition the media.

In lieu of mature adipocytes, many groups utilize the adipose precursor, adipose stromal cells (ASC). The use of ASCs allows the propagation of adipose precursors and the differentiation of ASCs into mature adipocytes as needed. Both ASCs and mature adipocytes can be used to condition media in order to study adipose-derived cytokines *in vitro*. There are different ASC models preferred in *in vitro* adipose research. Some groups utilize the established murine pre-adipocyte line 3T3-L1 (41,42). Other groups use primary ASCs isolated from human patient adipose tissue (37, 43-44). There are advantages of using human ASCs because its use makes it possible to specifically study breast adipose tissue involved in differing states of carcinogenesis.

1.4.1.2 Adipose Stromal Cells

To date, the Seewaldt lab has 18 characterized ASC lines and over 30 additional lines that have yet to be characterized. Adipose stromal cells are isolated from primary patient adipose tissue and characterized by their ability to differentiate and their cytokine profile in conditioned media. Freshly isolated ASCs are maintained in culture until multiple passages are frozen at -80^{o}C.

Breast adipose stromal cells are utilized because of their importance to the breast microenvironment. Thus, all of the ASC lines are derived from prophylactic mastectomies or mastectomies as a result of a cancer diagnosis. Depending on the nature of the surgery and the ability to successfully isolate ASCs, there are ASC lines for both breasts from the same women, allowing for potential studies comparing diseased breast tissue to non-diseased breast tissue.

1.4.1.3 ASC Characterization

The 18 ASC lines of the study came from a panel of women whose body mass index (BMI) ranged from 22-44 and whose age ranged from 32-45. Three of the women were also BRCA1 mutation carriers. Two ASC lines were produced from each breast of one of the women carrying a BRCA1 mutation, thus generating four lines that carry a BRCA1 mutation.

To characterize these the ASCs, these cell lines were differentiated into adipocytes and osteocytes to show pluripotency, which is characteristic of ASCs. The IL6 levels were then measured in conditioned media using ELISA (Figure 1). Not all of the cell lines were differentiated into either adipocytes or osteocytes. The inability to differentiate could be due to different factors. Firstly, fibroblasts could have grown out of the ASC isolation. Fibroblasts are visually the same as ASCs, and both have similar cell surface markers, which make them impossible to sort. One way to test if there is fibroblast contamination is to quantify the collagen mRNA in the non-differentiating ASCs. Fibroblasts will upregulate collagen mRNA while ASCs will not. Secondly, the ASCs may not have the ability to differentiate because of unforeseen signaling that inhibits ASC differentiation. For example, TGF-β inhibits ASCs from differentiating into adipocytes (45). Thus, in order to elucidate why all of the cells did not differentiate properly, further characterization will be necessary.

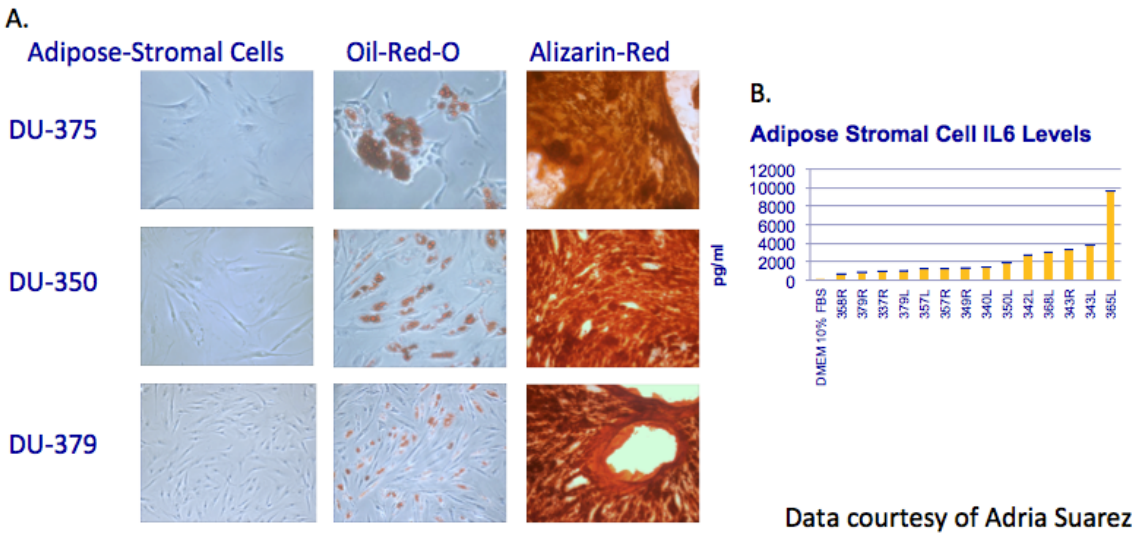

Figure 1: Adipose stromal cell characterization

Adipose stromal cells are isolated from breast adipose tissue of women who are at high risk for breast cancer yet are without disease. A) Bright field images of ASCs from three different patients in their undifferentiated form, differentiated into adipocytes and stained with Oil-Red-O, or differentiated into osteocytes and stained with Alizarin-Red. B) Characterization of secreted IL6 levels from 14 primary ASC lines generated. Note the varying range of IL6 production from cell lines. 4 of the 5 highest producers are carriers of BRCA1 mutations.

The measured IL6 levels in 14 of the 18 characterized ASC cell lines ranged from 1 ng/mL to almost 10 ng/mL (Figure 1). Mature adipocytes and preadipocytes have been reported to secrete IL-6 (13-15, 35-37). Additionally, mature adipocytes and preadipocytes secret other cytokines (13, 35-36). A RayBiotech Human Inflammatory Cytokine Array and a Human Growth Factor Array were screened with ASC-conditioned media to determine which cytokines and growth factors were secreted in addition to IL6. There were no measurable growth factors secreted into the media, although multiple groups reported ASCs secreting VEGF, HGF, and M-CSF into the media (13, 39). The Human Inflammatory Cytokine Array did confirm the presence of IL6 and IL8 (Figure 2). Two other cytokines were present: tissue inhibitor of metalloproteinases 2 (TIMP-2), and monocyte chemoattractant protein-1 (MCP-1). TIMP-2 inhibits metalloproteinases and MCP-1 was discovered as a chemokine for monocytes (46-47). There was no measurable IL1β or TNFα (Figure 2). Published studies, however, have shown that both of these cytokines are secreted by ASCs (13, 39).

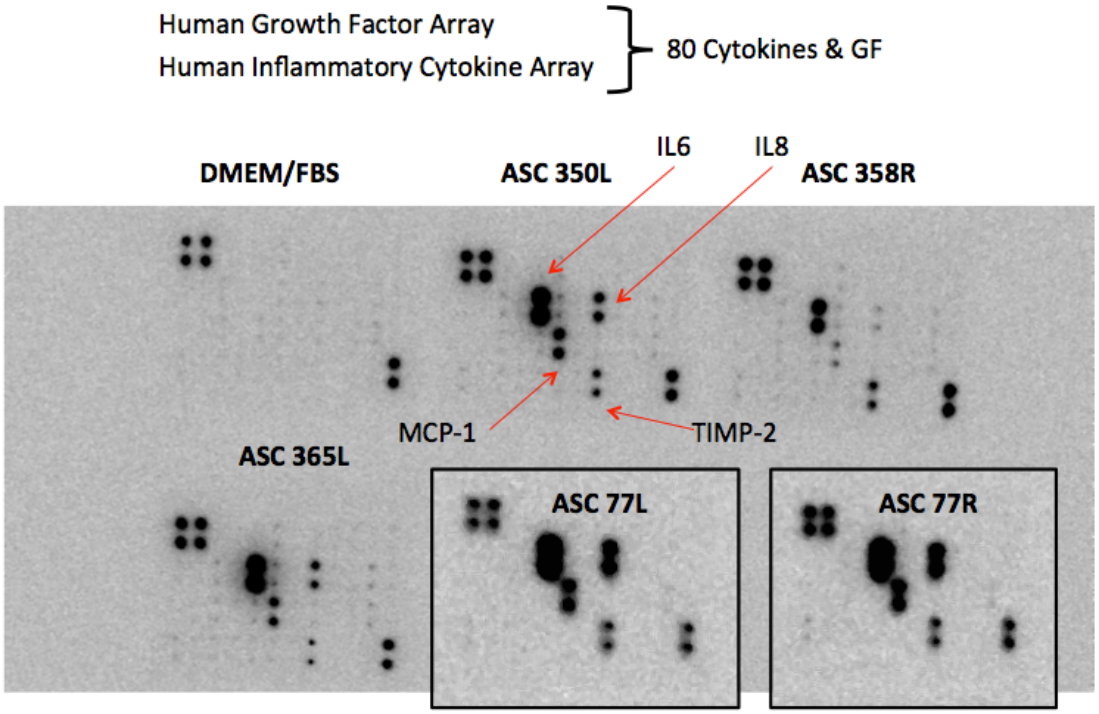

Figure 2: Adipose stromal cell cytokine characterization

Two RayBiotech Cytokine Arrays were used to characterize the ASC-conditioned media. Human Inflammatory Cytokine Array is pictured above. Each of the six conditioned media had measureable levels of IL6, IL8, MCP-1, and TIMP-2. The remaining dots were positive controls. The Human Growth Factor Array did not produce any measureable results.

A Luminex® Multiplex Cytokine Assay was performed to confirm quantitatively the levels of IL6, IL8, and MCP-1, and to confirm the absence of TNFα, TGFβ, and IL1β. This method uses less conditioned media, is more sensitive, and has a broader range allowing for detection of lower and higher concentrations of cytokine than an ELISA. The data confirmed the presence of IL6, IL8, and MCP-1, and they provided a quantitative measurement of each cytokine present in the respective ASC-conditioned media (Figure 3). The data also confirmed the absence of TNFα, TGFβ (Figure 3), and IL1β (data not shown).

Primary adipose-conditioned media were measured for the levels of IL6, IL8, and MCP-1 using the multiplex assay to show that the ASCs are producing levels of cytokines similar to those produced by primary adipocytes. The IL6 and IL8 produced a wide range of concentrations across the primary adipose-conditioned media samples, but MCP-1 had a much smaller range of concentrations (Figure 3). IL6 and IL8 produced by the ASCs fell within the range of IL6 and IL8 concentrations produced by the primary adipose tissue. The MCP-1 in the ASC-conditioned media was approximately 50% of the MCP-1 produced by the primary adipose tissue.

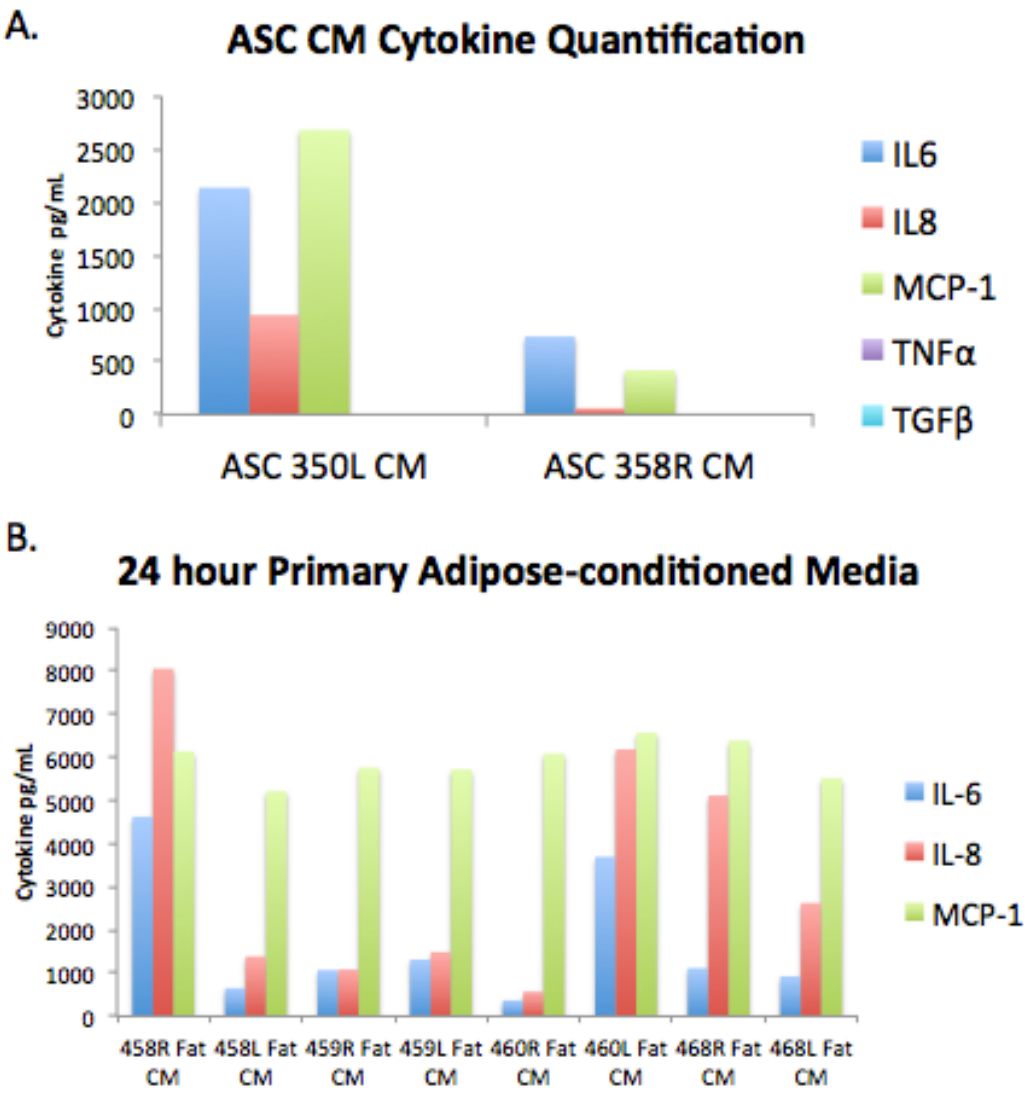

Figure 3: Conditioned media cytokine quantification using Luminex® Multiplex Cytokine Assay

Luminex® Multiplex Cytokine Assay was used to quantify the amount of cytokines present in conditioned media and to verify the absence of specific cytokines. A) The multiplex data confirms that the adipose stromal cell conditioned media do contain IL6, IL8 and MCP-1, and that they do not contain TNFα or TGFβ. B) Conditioned media taken directly from adipose cubes incubated in media for 24 hours confirm that the adipose tissue produces IL6, IL8, and MCP-1.

1.4.1.4 Optimizing ASC-conditioned Media

Adipose stromal cell conditioned media has been used extensively *in vitro* with transformed cells. The use of ASC-conditioned media with most transformed cells is simple because both cell types are grown in media containing fetal bovine serum (FBS). Non-transformed cells are not grown in media containing FBS. MCF10A cells, for example, are grown in media containing adult horse serum (HS), which does not have the same growth factors as FBS. MCF10A is a non-transformed, spontaneously immortalized epithelial cell line derived from a woman who had fibrocystic disease (48). It is a widely used and well-characterized epithelial cell line. MCF10A is an ideal non-transformed, mammary epithelial cell model because of its ability to undergo EMT and its use in a 3D modeling system (26, 33, 60, 63).

Adipose stromal cells were tested to determine if they could be grown with horse serum instead of FBS. The cells were grown in DMEM with 5% HS or DMEM/F12 with 5% HS, and their growth was measured by an MTT viability assay. The results of the experiment suggest that horse serum retarded the growth of ASCs (Figure 4). There were also fewer visible cells in the DMEM/F12 with 5% HS condition. When measured using a RayBiotech dot array, the cells in the horse serum still produced the same cytokine profile as those grown in FBS (Figure 4). Though the cells produced a similar cytokine profile, the horse serum prevented the differentiation of the ASCs into adipocytes or osteocytes (Figure 5). The cells grown in DMEM with 5% HS were not stained by Oil-Red-O or Alizarin Red, indicating that they did not undergo adipogenesis or osteogenesis respectively. The cells grown in DMEM/F12 with 5% HS lifted from the

plate during the incubation in both differentiation medias. Thus, data were not acquired from DMEM/F12 with 5% HS condition (Figure 5). Therefore, moving forward, conditioned media containing FBS were used to test the MCF10A cells during *in vitro* experiments.

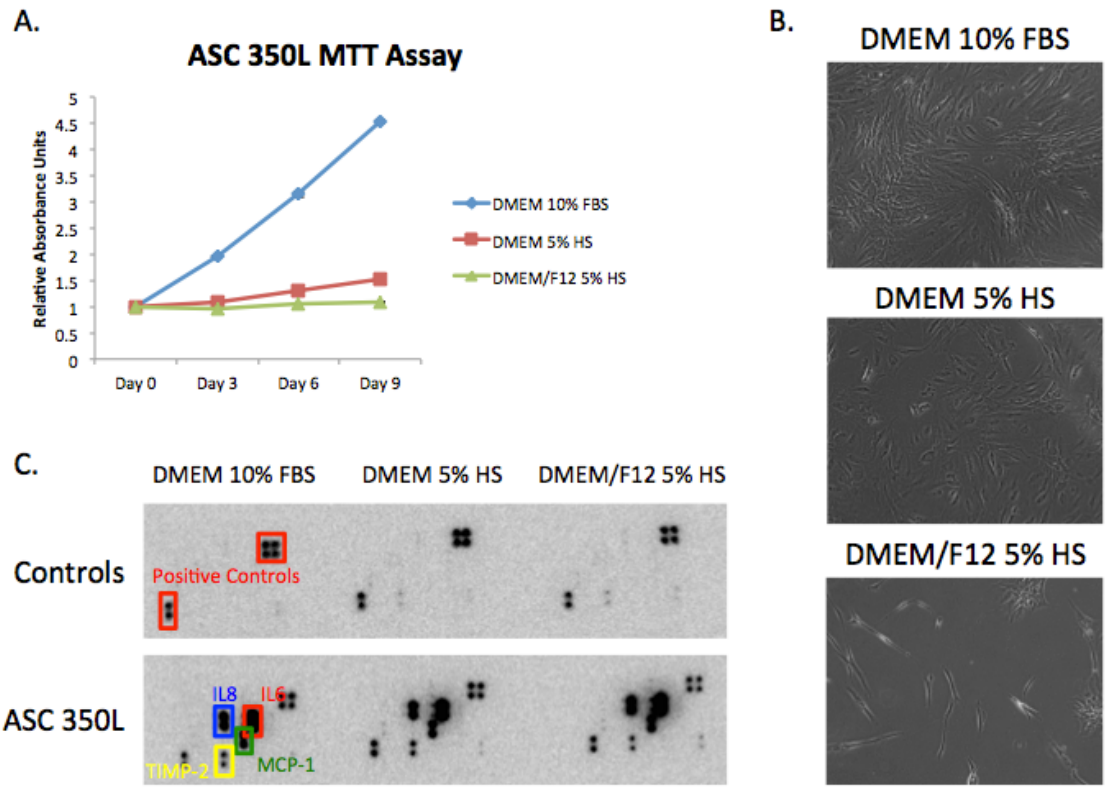

Figure 4: Horse serum slows the growth of adipose stromal cells.

Adipose stromal cells are cultured in DMEM salts media with high glucose and 10% FBS. Non-transformed, mammary epithelial cells, MCF10As, are grown in DMEM/F12 supplemented with horse serum and additional growth factors. ASCs were tested to determine if they could be grown under the same conditions as MCF10A cells. A) An MTT assay measured ASCs grown under three different conditions. The presence of horse serum (HS) significantly retards cell growth. B) Additionally, brightfield images of the cell numbers at the end of the nine days show how few cells were in either horse serum condition. C) ASCs produced IL6, IL8, MCP-1 and TIMP-2 under all conditions when tested with a RayBiotech Human Inflammatory Cytokine Array.

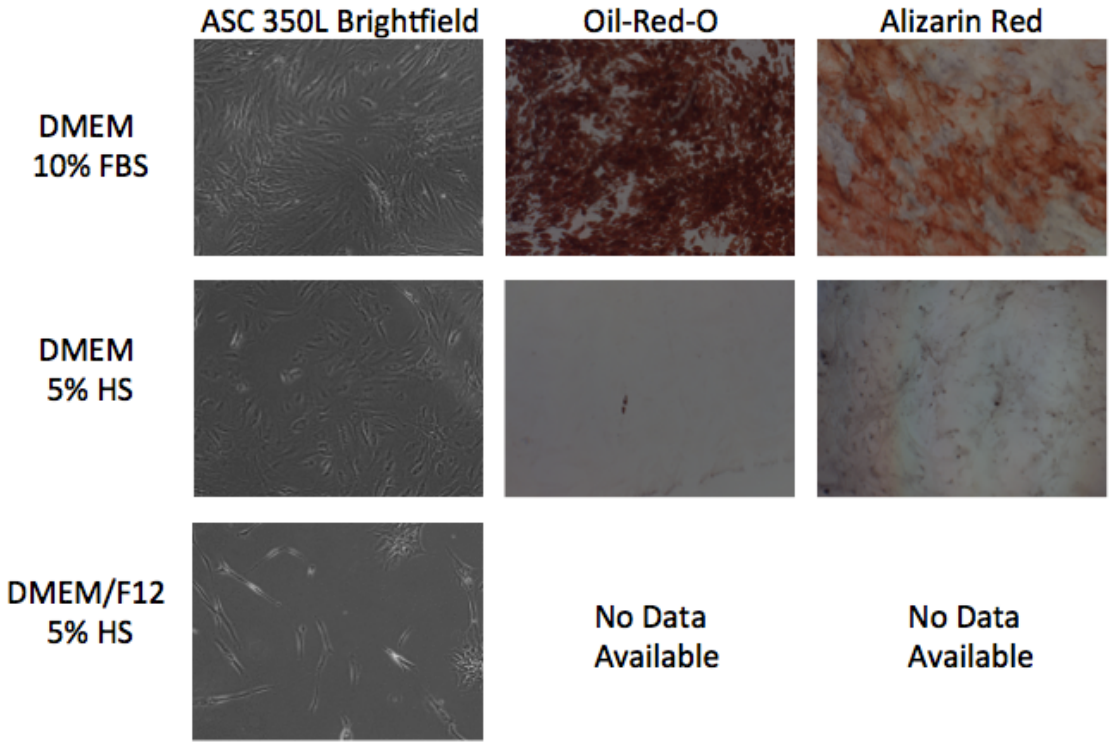

Figure 5: Horse serum prevents the differentiation of ASCs into adipocytes and osteocytes

ASCs were seeded at the same confluency. Once the control cells (DMEM 10% FBS) reached 100% confluency, the cells were treated with adipogenic, osteogenic, or normal growth media for suggested length of differentiation. Adipocytes were stained with Oil-Red-O and osteocytes were stained with Alizarin Red. The DMEM containing horse serum (HS) did not differentiate into mature adipocytes or osteocytes. No data were available for DMEM/F12 with horse serum because the sparse cells lifted during the differentiation process.

1.4.1.5 ASC & MCF10A Co-culture

When cultured with ASC-conditioned media for two weeks, MCF10A cell morphology changed. Furthermore, ASC-conditioned media increased Vimentin by western blot, and increased wound closure by wound healing migration assay (Figure 6).

The ASC-conditioned media had multiple factors present: IL6, IL8, and MCP-1. IL6 has been shown to induce EMT in transformed breast cells (27, 37). Blocking IL6, using antibodies, from the conditioned media did not inhibit Vimentin protein increase, and treating with recombinant IL6 did not increase Vimentin protein. Additionally, IL8 has been shown to induce EMT in breast cancer cell lines (30). Treatment of MCF10A cells with recombinant IL8, however, did not induce Vimentin protein. MCP-1 has not been shown to induce EMT in mammary epithelial cells, but MCP-1 in kidney and peritoneum EMT has been studied. Because of its role in kidney and peritoneum EMT, MCP-1 may potentially induce EMT in mammary epithelial cells.

Quantitative measurement, using a Luminex® Multiplex assay, of the 24 hour conditioned media taken off of the MCF10As at day 7 and day 14 revealed an increase in the concentration of IL8 and MCP-1 in the media (Figure 7). ASC-conditioned media contributes paracrine MCP-1, but these data suggest that the MCF10As begin secreting MCP-1 into the media in an autocrine manner.

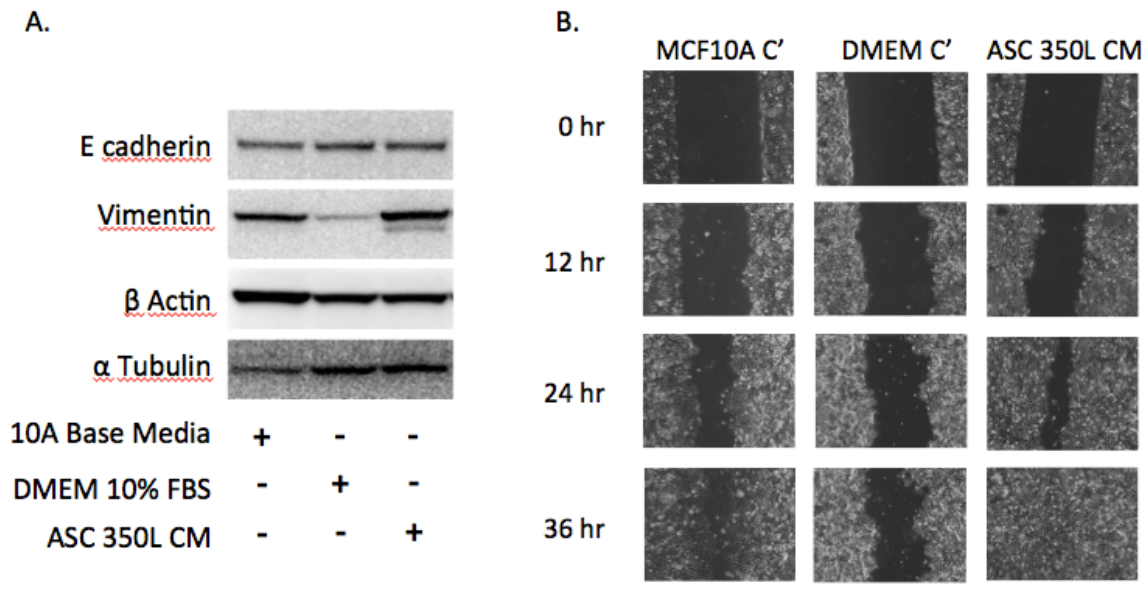

Figure 6: ASC-conditioned media induces Vimentin and increases migration

MCF10A cells were grown in DMEM/F12 5% HS (base media), DMEM 10% FBS, and ASC-conditioned media for two weeks. A) Conditioned media induced Vimentin protein expression in MCF10A cells. B) Conditioned media increased migration by scratch assay in MCF10A cells.

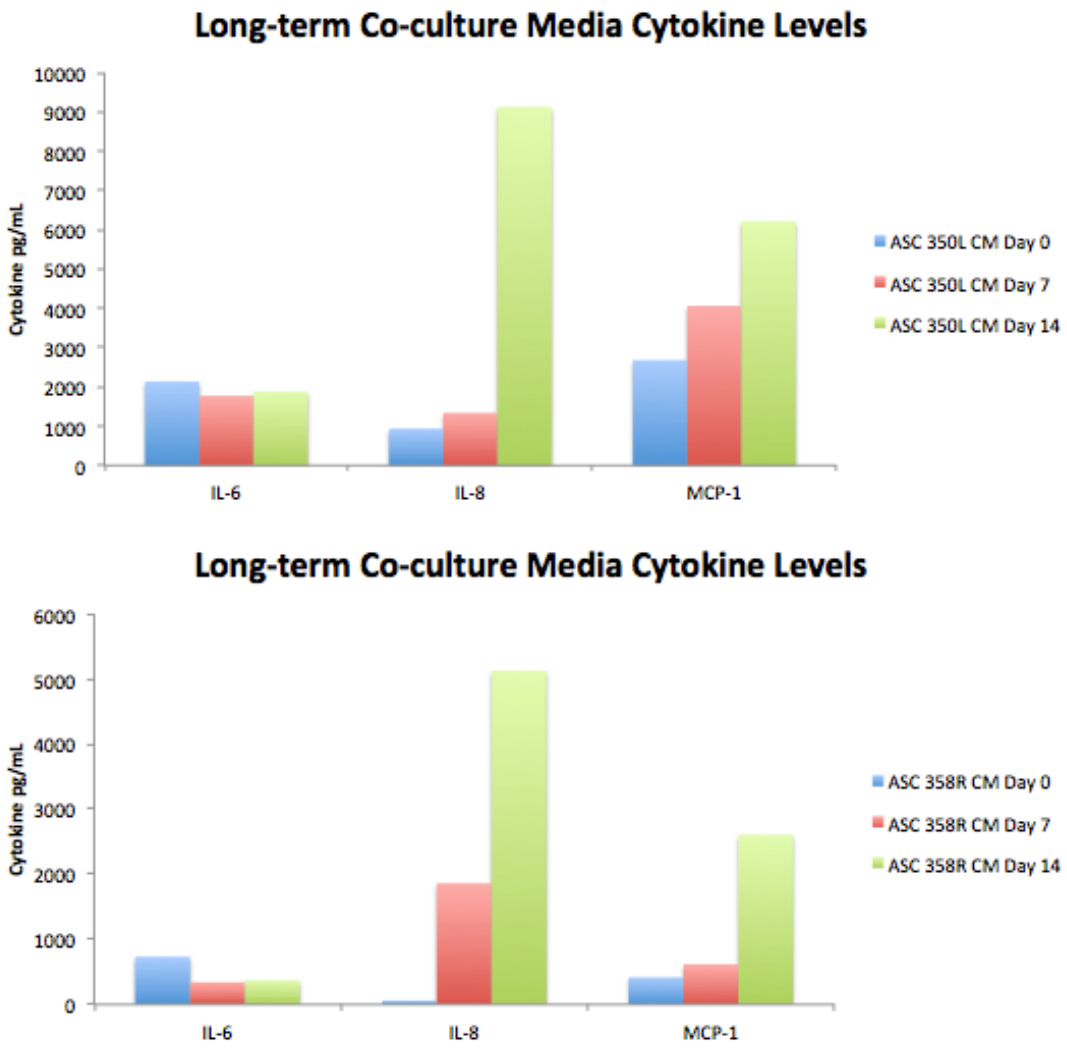

Figure 7: Long-term co-culture with ASC-conditioned media induces IL8 and MCP-1 secretion by MCF10A cells

Passage-matched conditioned media saved either before they were used or 24 hours after they were used on cells. Media came from time points as indicated and were measured using Luminex® Multiplex Cytokine Array quantitative technology. MCF10A cells grown in conditioned media from two different ASC lines both secreted IL8 and MCP-1 into the media by Day 14.

1.5 Monocyte Chemoattractant Protein-1

Monocyte chemoattractant protein-1 is a small cytokine that belongs to the CC family of chemokines. Chemokines are chemotactic cytokines whose main function is to regulate cell trafficking and are secreted in response to signals such as proinflammatory cytokines (49). This chemokine induction could explain why the MCF10As would start secreting MCP-1 and IL8 after treatment with ASC-conditioned media, which contain proinflammatory cytokines. Chemokines are grouped into two main functional subfamilies: inflammatory and homeostatic. Inflammatory chemokines control the recruitment of leukocytes to sites of injury and inflammation. Homeostatic chemokines perform housekeeping functions by navigating leukocytes between secondary lymphoid organs and within the bone marrow and thymus (49).

Outside of their normal immune roles, chemokines are involved in a number of diseases: autoimmune disorders, pulmonary disease, transplant rejection, vascular disease, and cancer. MCP-1 has been demonstrated as a potential intervention point for the treatment of multiple sclerosis, rheumatoid arthritis, and insulin-resistant diabetes (49). Additionally, MCP-1 has been implicated in kidney injury, fibrosis, and EMT, and MCP-1 has been implicated in peritoneal fibrosis and EMT. (78-79, 90-93). While it is amongst the most studied members of the chemokine family, the role of MCP-1 in breast cancer has only recently been brought to light.

MCP-1 is a potent regulator of the migration and infiltration of monocytes and macrophages. It is produced by a variety of cell types, either constitutively or after induction by cytokines or growth factors. These include endothelial, fibroblastic,

epithelial, smooth muscle, mesangial, astrocytic, monocytic, and microglial cells (49). An increase in adipose tissue is a major contributor to increased MCP-1 levels in the human body. Multiple groups have shown that circulating concentrations of MCP-1 correlated positively with adiposity (50-51). It was also shown that insulin increased the concentration levels of MCP-1 secreted by adipocytes (50). Taken together, obesity is associated with increased MCP-1.

1.5.1 MCP-1 Signaling

Chemokines signal cells by binding and activating G-protein-coupled receptors (GPCRs) (49). The primary receptor for MCP-1 is CCR2 (49), but models of CCR2 knock-out mice and cells used from those mice suggest other possible receptors (52-53). The chemokine receptor CCR4 has been shown to bind MCP-1 and mediate migration in cells lacking CCR2 (54-55). Both transformed and non-transformed breast cell lines express varying levels of CCR2 protein and mRNA (Figure 8). Upon binding together of MCP-1 and CCR2, the mitogen–activated protein kinase (MAPK) signaling pathway is activated through Ras/Raf/Mek signaling. Activation of Ras/Raf/Mek signaling results in phosphorylation of Erk1/2 at T202/Y204 (53, 56-58). MCF10A cells treated with MCP-1 rapidly phosphorylate Erk1/2 at T202/Y204, but this activation is lost by 24 hours (Figure 9). IL6 is an inflammatory cytokine capable of activating Erk *in vitro* (80). IL6, however, activates JAK-STAT signaling, which results in Stat3 phosphorylation at Y705 in MCF10A cells (Figure 9).

Taken together, MCP-1 is an inflammatory chemokine that correlates with obesity, activates Erk MAPK signaling, and induces kidney and peritoneum EMT. It

remains to be determined if MCP-1 directly induces EMT in non-transformed, mammary epithelial cells.

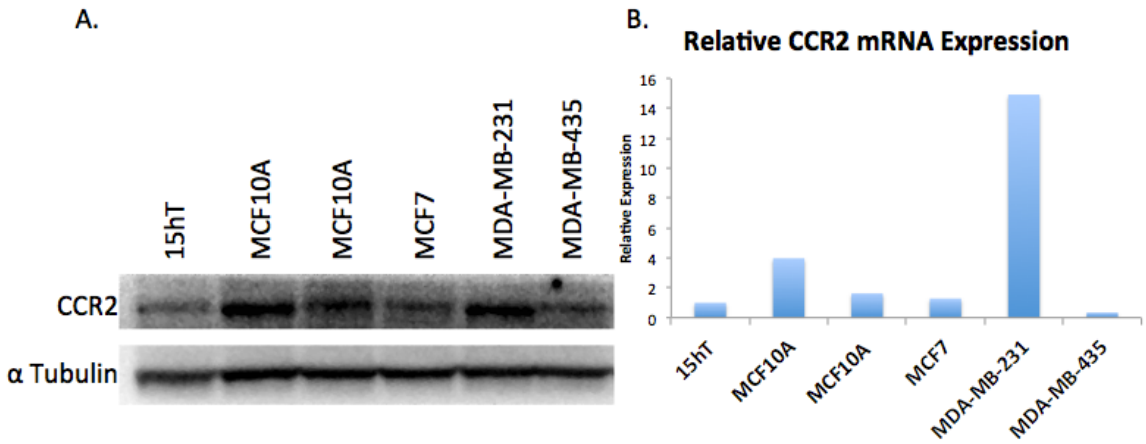

Figure 8: CCR2 quantification

The data above quantify the chemokine receptor CCR2 in several breast cell lines by A) western blotting and B) qRT-PCR. 15hT is an hTERT immortalized non-transformed human mammary epithelial cell (HMEC). There are two MCF10A cell lines compared here. While both are MCF10A, their culturing history has resulted in modified CCR2 levels. MCF7 cells are from a luminal breast tumor while MDA-MB-231 and 435 are both TNBC cell lines.

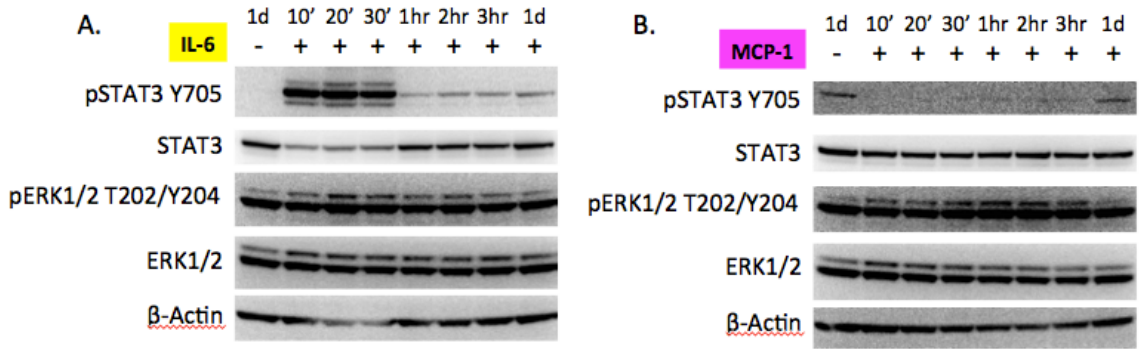

Figure 9: Cytokine signaling pathway activation

MCF10A cells were treated with either 20 ng/mL IL6 or MCP-1, and protein lysates were extracted at the time point indicated. A) IL6 binds IL6 receptor, signals through GP130 and rapidly phosphorylates STAT3 at Y705. B) MCP-1 binds CCR2, activating MAPK signaling through Ras/Raf/Mek, which results in phosphorylation of ERK1/2 at T202/Y204.

2 Materials and Methods

2.1 Antibodies and Reagents

Anti-Vimentin (Rabbit), -p44/42 MAPK, -phospho p44/42 MAPK(T202/Y204), -αTubulin, -Cleaved Caspase 3, -CCR2, -βcatenin, -Stat3, and -phospho STAT3(Y705) were purchased from Cell Signaling. Anti-Vimentin (Mouse), -Ncadherin, and -Ecadherin, were purchased from BD Bioscience. Anti-Integrin α6, or HRP conjugated Actin, donkey anti rabbit, and donkey anti mouse were purchased from Santa Cruz. Alexa Fluor anti-mouse 594 nm and anti-rabbit 488 nm were purchased from Life Science Technologies. APC, APC-CD44, PE, and PE-CD24 were purchased from BD Pharmigen.

Recombinant human IL6, IL8, MCP-1, and MMP-2; and Quantikine Human IL6 ELISA were purchased from R&D Systems. Human TGF-β1, TNFα, and PD98059 were purchased from Cell Signaing. Thiazolyl Blue Tetrazolium Bromide and Eosin Solution were purchased from Sigma Aldrich. Hematoxylin was purchased from Lerner Laboratories. Normal goat serum and Immunofluorescence mounting solution were purchased from Vector. DAPI, NuPAGE 4-12% Bis-Tris Gel, NuPAGE MOPS SDS Running Buffer, Novex 10% Zymogram (Gelatin) Gel, Tris-Glycine SDS Running Buffer, Novex Zymogram Renaturing Buffer, Novex Zymogram Developing Buffer, and Tris-Glycine Sample Buffer were purchased from Life Science Technologies. 8.0 micron, 6.5 mm PET membrane inserts were purchased from COSTAR. Transcriptor First Strand cDNA synthesis kit was purchased from Roche. RT^2 SYBR Green qPCR Mastermix, Prevalidated human CCR2 qPCR primers, and RNeasy Plus Mini Kit were purchased

from Qiagen. Milliplex plates for Luminex were purchased from EMD Millipore. Growth factor reduced Matrigel and Dispase were purchased from BD Bioscience. Bio-Safe Coomasie protein stain was purchased from BioRad.

DMEM, DMEM/F12, FBS, and 0.5% Trypsin-EDTA were purchased from Gibco. Hydrocortisone and Insulin were purchased from Sigma Aldrich. Cholera Toxin was purchased from Calbiochem and EGF was purchased from Peprotech.

2.2 ASC-conditioned Media

Adipose Stromal Cells were seeded at 1.4 x 10^6 in 20.6 mL of DMEM media supplemented with 10% FBS in a T75 flask. After 72 hours, the media was removed from the cells and spun down at 1200 rpm. The supernatant was frozen at -80^{o}C in 10 mL aliquots and never thawed more than twice.

2.3 Long-term 2D Co-culture

MCF10A cells were seeded at 6 x 10^5 in 3 mL of media in a T25 flask. The medias the cells were cultured in are described in Table 1. The media were changed every 24 hours for the length of the experiment. Every three days the cells were reseeded (Figure 10). On day 12, MCF10A cells were seeded at 4 x 10^5 in 2mL media in duplicate in a 6 well plate for protein lysates.

Table 1: Medias used in long-term 2D co-culture

Listed below are the nine conditions used in the 2D long-term co-culture experiment. Both TGF-β1 and TNFα were used as positive controls for EMT. The TGF-β1 control was removed after the four days because the cells were arresting and TNFα was a better long-term control. All medias were supplemented with EGF, Hydrocortisone, Insulin and Cholera Toxin.

DMEM/F12 + 5% Horse Serum	**DMEM + 10% FBS**
Untreated	Untreated
2ng/mL TGF-β1	2ng/mL TGF-β1
4ng/mL TNFα	4ng/mL TNFα
20ng/mL MCP-1	20ng/mL MCP-1
	ASC-conditioned Media

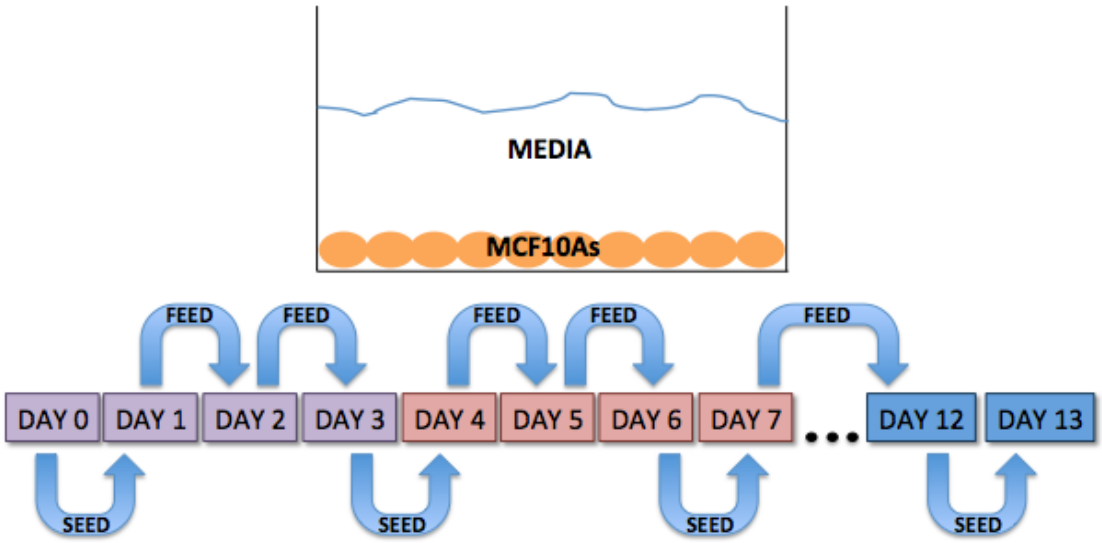

Figure 10: Schematic of long-term 2D co-culture work flow

The cells were seeded on Day 0 and reseeded at days 3, 6, 9 and 12 to prevent the MCF10As from becoming confluent. The media was changed every 24 hours to maintain constant cytokine signaling.

2.4 Long-term 3D Culture

MCF10A cells were seeded at 5 x 10^2 in 200μL assay media per well in an 8 well chamber slide coated with 100μL growth factor reduced Matrigel. Acini were allowed to form for 14 days with regular media changes every 2-3 days. On the day 14, the media was removed and replaced with fresh media containing: 5ng/mL MCP-1; 10μM PD98059; MCP-1 & PD98059; or nothing (untreated control). These medias were changed every 24 hours for 4 days. On day 18, the chamber slides were processed for immunofluorescence.

2.5 Migration & Invasion Assays

2.5.1 Boyden Chamber Migration Assay

MCF10A cells were seeded at 2 x10^4 in 100μL of base media or base media containing 10μM PD98059 into the upper chamber of a 6.5 mm 8μm PET Boyden Chamber and allowed to incubate at room temperature for 30 min. The upper chamber was then placed into a well containing 600μL of base media containing: 5ng/mL MCP-1; 10μM PD98059; MCP-1 & PD98059; or nothing (untreated control). The Boyden Chambers were placed at 37°C, 5% CO_2, and humidity for 21 hours.

After the overnight incubation, the upper chambers were removed and washed twice with PBS and fixed in 2% buffered formalin for 10 min. The cells inside the upper chamber were removed with a cotton swab. The cells on the bottom of the membrane were stained for 10 min in hematoxylin, washed 3 times in dH_2O, counter stained for 10 min in eosin, and washed 3 times in dH_2O. Cells were then imaged at 10x on a Zeiss

inverted light microscope. Five images per membrane were taken and the average number of cells per field of view were recorded.

2.5.2 Spheroid Gel Invasion Assay

MCF10A cells were seeded at 2.4 x 10^4 cells per well in a 6 well plate embedded in 800μL of growth factor reduced Matrigel. 2 mL of assay media was added to each well after the gels polymerized and speroids were allowed to form for 14 days with regular media changes every 2-3 days. On the day 14, the media was removed and replaced with fresh media containing: 5ng/mL MCP-1; 10μM PD98059; MCP-1 & PD98059; or nothing (untreated control). These medias were changed every 24 hours for 4 days. On day 18, spheroids were imaged using light microscopy. The media was spun down at 1200 rpm and the supernatant was used for gelatin zymography.

2.6 Immunofluorescence

Media was removed from each chamber well and the cells were washed once with ice-cold PBS. Cells were then fixed in ice-cold methanol and incubated at -20°C for 10 min. Cells were then washed twice with room temperature PBS and incubated in blocking solution (5% BSA, 0.05% Triton, PBS, 1:500 normal goat serum) for 30 min at room temp. Cells were then incubated in primary antibody overnight at 4°C while rocking.

The following day, cells were allowed to warm to room temperature for 60 min and washed twice with PBS. Secondary antibodies were added at 1:400 in PBS and incubated for 60 min at room temperature in the dark. The secondary antibodies were then removed and the cells were stained with DAPI (1:5000 in PBS) for 3 min at room

temperature and then washed twice with PBS. Cells were then mounted using Vector immunofluorescent mounting solution and a coverslip, dried, and stored at 4°C prior to imaging. All images were taken with a Zeiss upright confocal microscope.

2.7 Gelatin Zymography

Media was removed from spheroid gel invasion assay after 24 hours of conditioning on the last day of treatment, spun down, and stored at -80°C or used immediately. 15µL of conditioned media was added to 15µL of 2x Tris-Glycine SDS loading buffer and 25µL of sample was loaded into each lane of a 10 well, 1.0 mm, Novex Zymogram (Gelatin) gel. One lane contained MMP-2 recombinant protein as a positive control. The samples were run at 150V until the dye front migrated off the gel. The gel was removed an incubated in Novex Zymogram renaturing buffer for 60 min at room temperature followed by an incubation in Novex Zymogram developing buffer for 60 min at room temperature. After the last incubation, the developing buffer was replaced and the gel was incubated for 18 hours at 37°C with humidity. The following day, the gel was washed in dH_2O and then stained for 60 min in Bio-Safe Coomasie protein stain. The gel was then destained in dH_2O for 60 min and imaged using a Kodak imager.

2.8 ASC Lineage Induction

ASCs were plated in 6 well plates and grown to confluency. For adipogenesis, the growth media was removed and replaced with adipogenic media (DMEM, 10% FBS, 0.5 mM IBMX, 1 µM dexamethasone, 10 µM insulin, 200 µM indomethacin) for two weeks changing the media every three days. To verify adipogenesis, cells were stained

with Oil-Red-O. For osteogenesis, the growth media was removed and replaced with osteogenic media (DMEM, 10% FBS, 0.1 μM dexamethasone, 50 μM L-ascorbic acid 2-phosphate, and 10 mM β-glycerophosphate) for three weeks changing the media every three days. To verify osteogenesis, the cells were stained with Alizarin Red.

2.9 Direct 3D Co-culture

ASCs were seeded and grown to confluency in 4 well chamber slides. Once they were confluent, 250 μL Matrigel was placed over the cells and solidified at 37°C. MCF10A cells were then seeded at 1×10^3 in 500 μL of media. The cells were allowed to grow for two weeks with fresh media every 2-3 days. After 14 days, the cells were processed for immunofluorescence.

3 Results

3.1 MCP-1 does not induce EMT in MCF10A cells in 2D culture

A 13-day culture was performed to determine whether MCP-1 induced EMT in MCF10A cells. After 13 days of culturing, the positive control TNFα abolished the expression of E-cadherin in the MCF10A cells (Figure 11). TNFα did not increase Vimentin or N-cadherin compared to the DMEM 10% FBS plus growth factor untreated control. ASC-conditioned media also did not increase Vimentin, which was observed in the initial co-culture. ASC-conditioned media did decrease E-cadherin compared to the DMEM 10% FBS control. The absence in Vimentin change could be due to the high basal levels of Vimentin in the cells after the culturing process. Both the TNFα and the ASC-conditioned media decreased the epithelial marker, E-cadherin. MCP-1 treatment did not decrease E-cadherin compared to the DMEM 10% FBS control, nor did it increase Vimentin or N-cadherin. Therefore, in 2D culture, MCP-1 does not induce EMT.

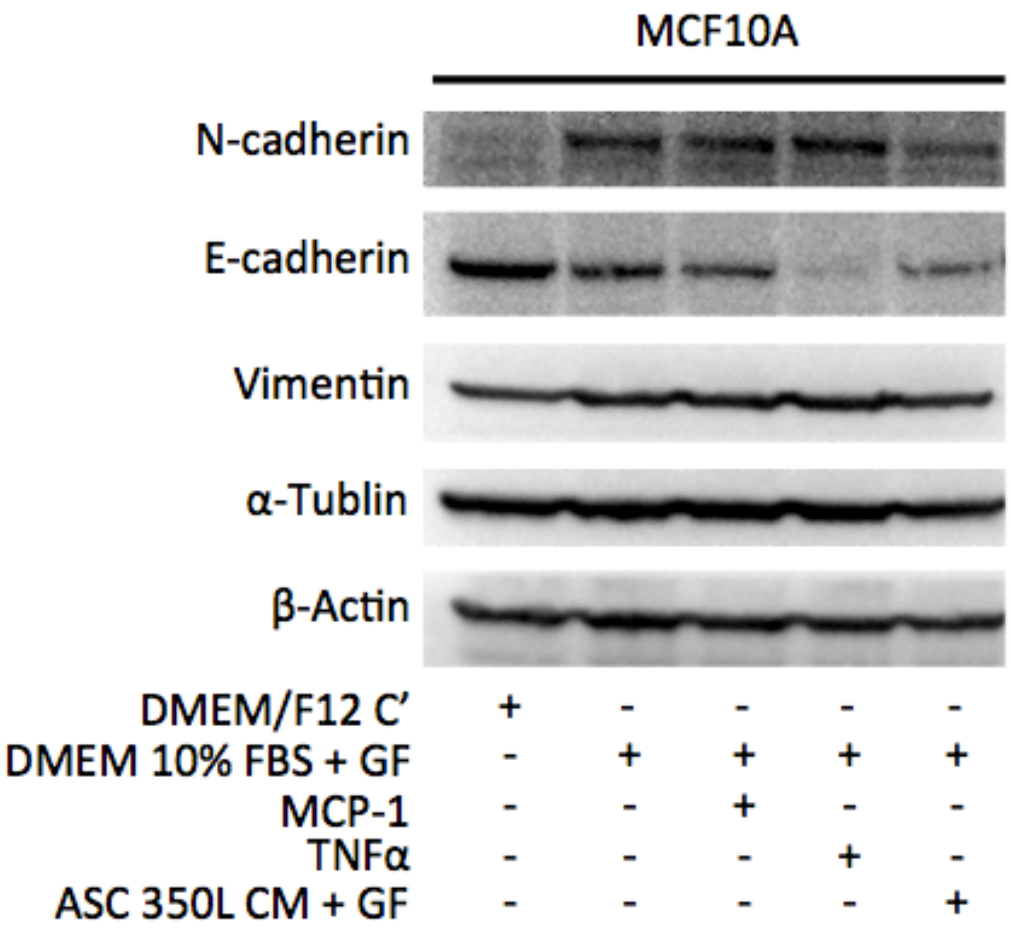

Figure 11: In 2D culture, MCP-1 does not decrease E-cadherin in 13 days

MCF10A cells treated for 13 days with MCP-1 did not decrease E-cadherin compared to the DMEM 10% FBS + Growth Factors (GF) control. TNFα treatment eliminated E-cadherin while ASC-conditioned media decreased E-cadherin compared to the DMEM 10% FBS + GF control.

3.2 MCP-1 rapidly decreases E-cadherin in 3D culture

Breast epithelial cells *in vivo* do not grow in a flat monolayer on plastic. Breast epithelial cells *in vivo* engage with the extracellular matrix (ECM), are polarized, and form 3D branching structures. MCF10A cells are used to form 3D acini with hollow lumen when grown in ECM to model *in vivo* characteristics. Therefore, MCF10A acini were treated with MCP-1 to test whether MCP-1 could induce EMT in non-transformed, mammary epithelial cells.

The fully formed lumens of MCF10A acini were hollow. The MCF10A cells expressed plasma membrane localized E-cadherin and β-catenin. Additionally, they weakly expressed Vimentin. Lastly, Integrin α6 was localized to the basal membrane, which indicated basal polarity (Figure 12).

After four days of treatment with MCP-1, MCF10A cells rapidly lost E-cadherin expression (Figure 13). Additionally, MCP-1 induced the loss of β-catenin expression, and Integrin α6 broke down around the protrusions (Figure 13).

Erk signaling is linked to the loss of E-cadherin expression in EMT (61-62). The pharmacological Erk inhibitor PD98059 was used to test whether inhibition of Erk prevents loss of E-cadherin. Pretreatment with PD98059 prevented MCP-1 induced phosphorylation of Erk1/2 at T202/Y204 in MCF10A cells (Figure 14). Treatment of MCF10A acini with PD98059 alone did not affect the morphology of the acini, nor did it alter the E-cadherin staining. The staining of β-catenin was lost when treated with PD98059, but Integrin α6 still stained the basal pole of the cells in the acini (Figure 13).

Pretreatment of MCF10A acini with PD98059, followed by co-treatment with MCP-1 and PD98059, prevented the loss of E-cadherin, formation of projections, and the breakdown of Integrin α6 (Figure 13). Only β-catenin was not restored, and this staining was lost with the treatment of PD98059. These data suggest that the Erk signaling pathway is necessary for MCP-1 induced E-cadherin loss in 3D.

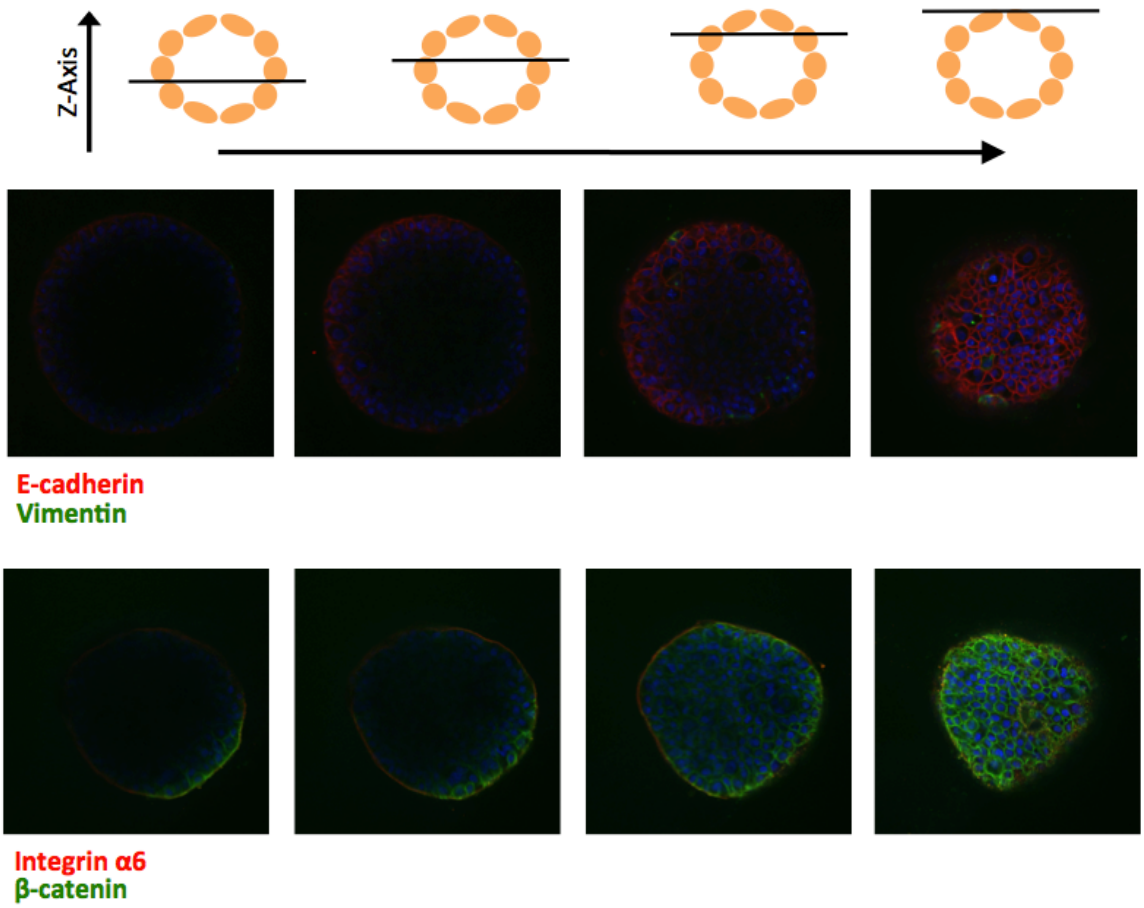

Figure 12: MCF10A cells form hollow acini when grown in Matrigel

MCF10A cells formed a hollow lumen when grown in a three-dimensional matrix. The epithelial cells expressed plasma membrane localized E-cadherin and minimal Vimentin. They also expressed plasma membrane localized β-catenin and Integrin $\alpha 6$.

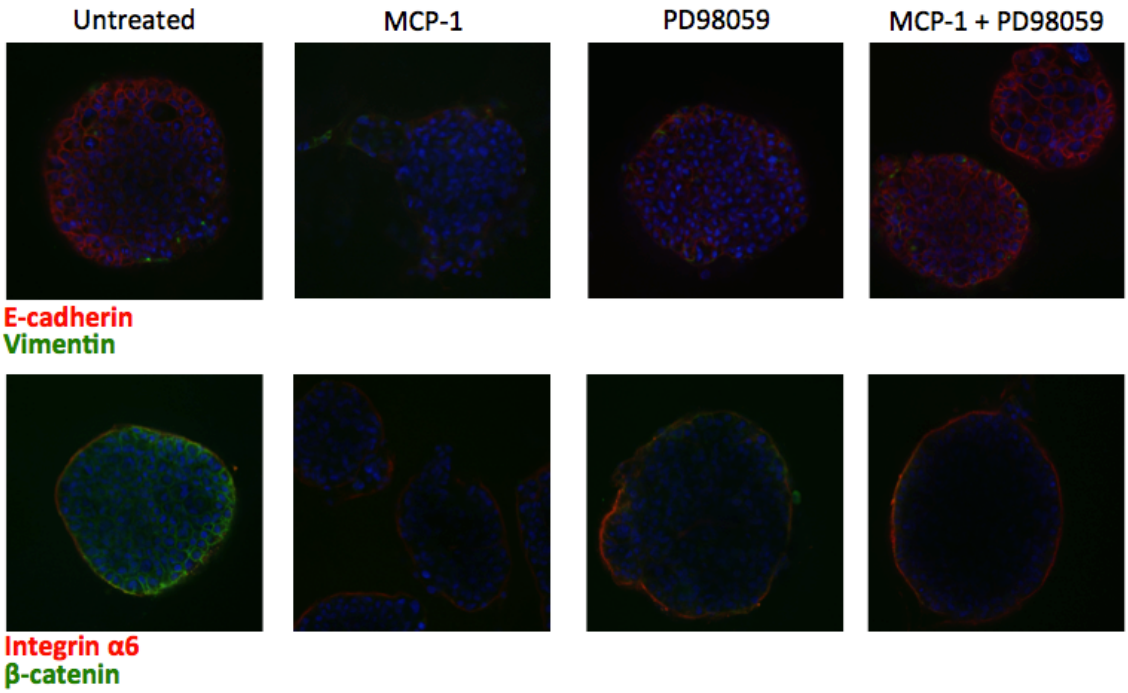

Figure 13: MCP-1 decreases E-cadherin and β-catenin in 3D

MCF10A cells were grown to form acini for 14 days and then treated for four days with MCP-1, PD98059, or both. MCP-1 caused a decrease in E-cadherin while PD98059 prevented loss of E-cadherin expression. MCP-1 also caused a breakdown of the basal polarity marker Integrin $\alpha 6$ expression and a loss in the epithelial marker β-catenin. The Erk inhibitor PD98059 also decreased β-catenin, and thus, did not prevent the decrease in β-catenin expression when treated with MCP-1.

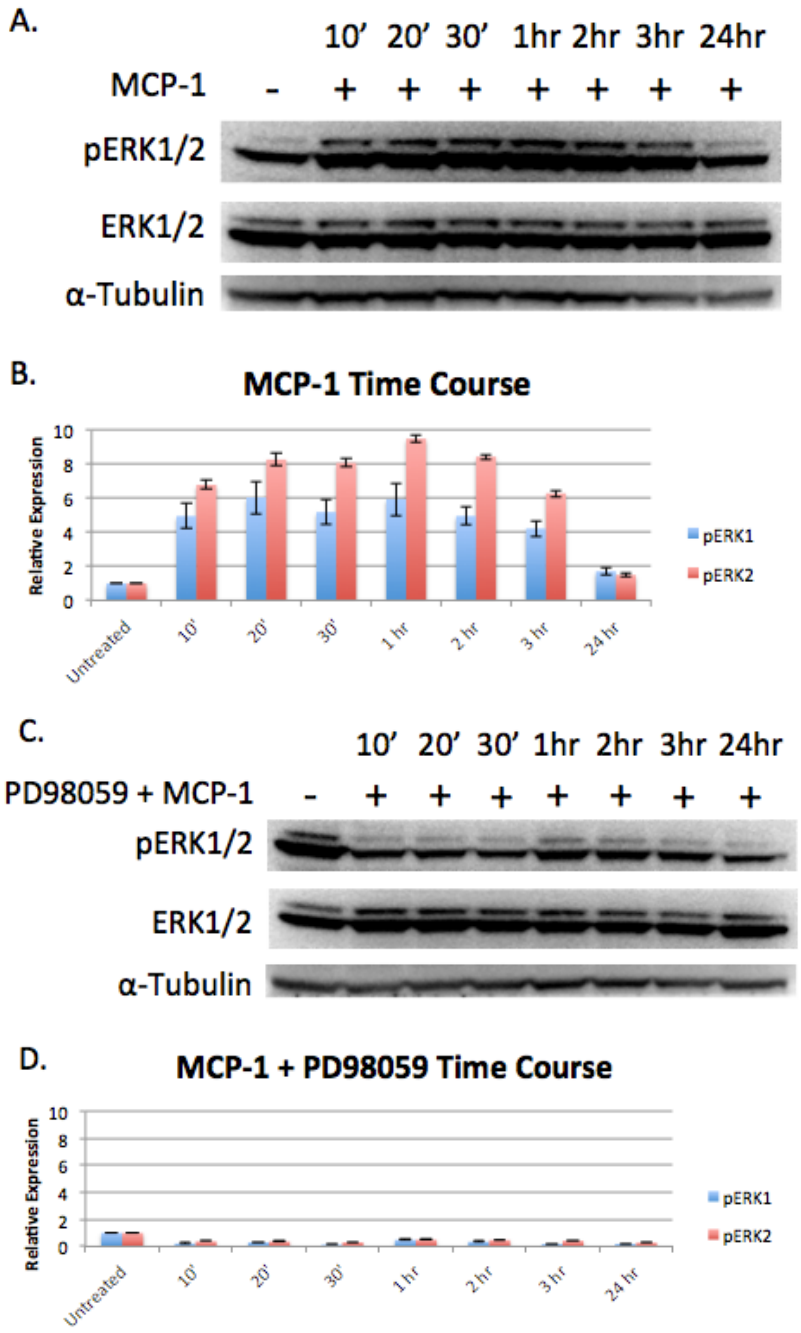

Figure 14: PD98059 blocks MCP-1 induced Erk1/2 phosphorylation

MCP-1 induced the rapid phosphorylation of Erk1/2, but this was blocked by the potent Erk inhibitor PD98059 at a concentration of 10 μM. A) Western blot of the MCP-1 time course. B) Quantification of relative expression of Erk1/2 phosphorylation over the MCP-1 time course. C) Western blot of the PD98059 + MCP-1 time course. D) Quantification of relative expression of Erk1/2 phosphorylation over the PD98059 + MCP-1 time course.

While the cells treated with MCP-1 appear to have lost their E-cadherin expression, it is possible that there was an excess of apoptosis in the E-cadherin expressing cells as a result of treatment. To rule this out, acini that went through the same 14-day growth and 4-day treatment process were dual-stained with cleaved Caspase 3 to indicate apoptosis and Integin α6 to indicate polarity and structure (Figure 15). There was minimal staining for cleaved Caspase 3 in all imaged acini. This includes MCP-1, PD98059, MCP-1 and PD98059, and untreated control. Joan Brugge's group showed that MCF10A cells will undergo apoptosis to form the hollow lumen (63). Therefore, the minimal cleaved Caspase 3 staining that occurred could be the remnants of cells clearing the lumen.

In summary, MCP-1 induced the loss of E-cadherin staining, the loss of β-catenin staining, and the loss of Integrin α6 staining surrounding the protrusions in MCF10A acini grown in 3D culture. Additionally, inhibition of Erk signaling with the pharmacological inhibitor PD98059 prevented these MCP-1 induced changes.

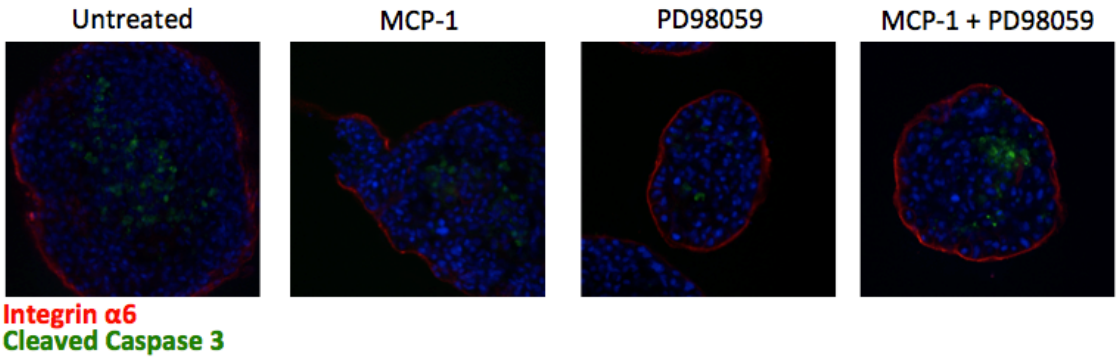

Figure 15: MCP-1 does not increase apoptosis within the acini

Acini were stained with cleaved Caspase 3 to rule out the loss of E-cadherin expressing cells by increased apoptosis. All acini in all conditions expressed some cleaved Caspase 3, but no more than any other condition. This is to be expected as MCF10A cells apoptose to clear the lumen, and cleaved Caspase 3 expression may remain because of clearing cells.

3.3 MCP-1 induces migration in MCF10A cells

A Boyden Chamber migration assay was used to determine whether MCP-1 induced chemotaxis of MCF10A cells. Untreated MCF10A cells did migrate, which was expected because studies have shown that MCF10As are migratory (33, 64). MCP-1, however, caused a 40% increase in migration of the MCF10A cells over that of the untreated controls (Figure 16).

MAP kinases govern cell migration, and Erk is rapidly phosphorylated by MCP-1 (65). Therefore, MCF10A cells pretreated with PD98059 were tested to determine whether they would migrate toward MCP-1 (Figure 16). When Erk signaling was inhibited, migration towards MCP-1 was significantly inhibited. These data suggest that MCP-1 increases MCF10A migration through an Erk signaling pathway.

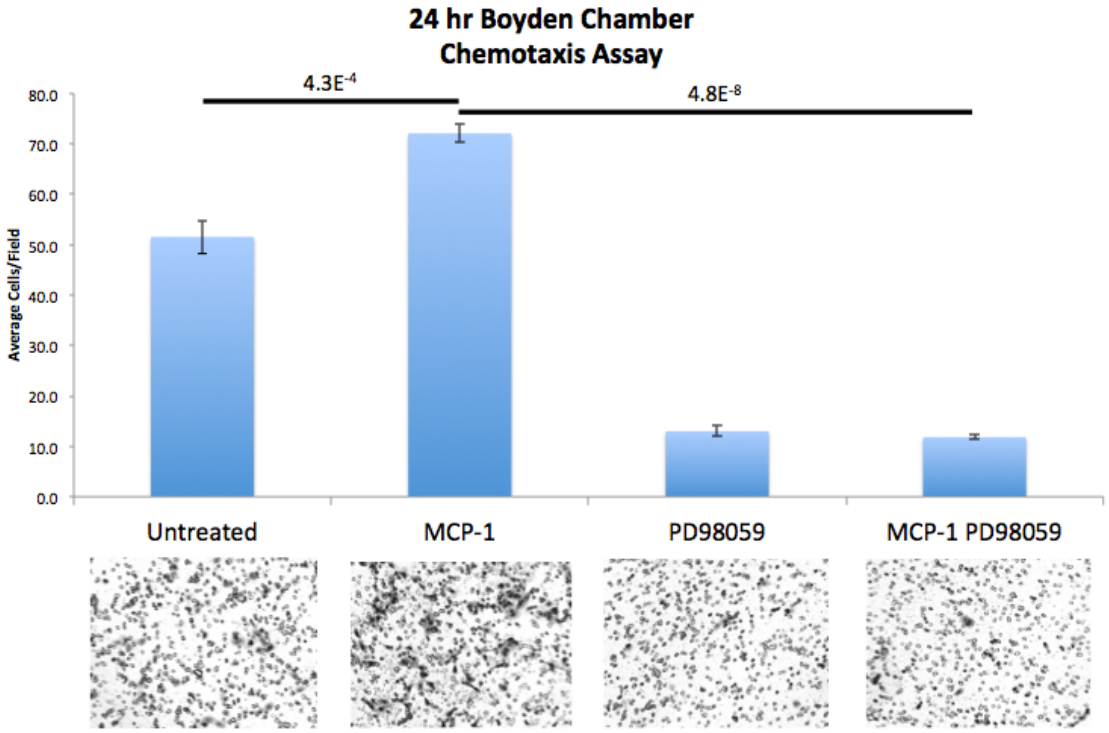

Figure 16: MCP-1 induces migration in MCF10A cells

In a Boyden Chamber migration assay, there was a 40% increase in migration in MCF10A cells when presented with MCP-1 as a chemoattractant. The Erk inhibitor PD98059 significantly decreased the migration of the cells and prevented the MCP-1 induced migration. Three independent experiments were conducted with two transwell Boyden Chambers per condition. P values were calculated using a student paired T-test with one-tailed distribution.

3.4 MCP-1 induces invasion in MCF10A cells

A spheroid gel invasion assay was used to test whether MCP-1 induced invasion in MCF10A cells. In this assay, non-invasive cell lines form compact spheroids with a distinct border when imbedded in 3D ECM. Invasive cells invade the surrounding matrix and display outgrowth from the spheroid. Invasion is then followed by live cell imaging (17).

MCF10A cells imbedded in ECM were grown for 14 days followed by 4 days of continuous treatment every 24 hours. Treatment of MCF10A spheroids with MCP-1 induced the invasion of cells away from the spheroids into the matrix (Figure 17). The distinct borders of the spheroids were lost as cells invaded the matrix and the cells invaded as clusters. In some instances, the cells passed through the matrix to populate the plastic chamberwell slide.

Pretreatment of MCF10A spheroids with the Erk signaling inhibitor PD98059 inhibited matrix invasion (Figure 17). Spheroids maintained their distinct borders and showed no signs of invasion. The inhibition of matrix invasion by PD98059 suggests that Erk signaling is necessary for MCP-1 induced invasion in MCF10A spheroids.

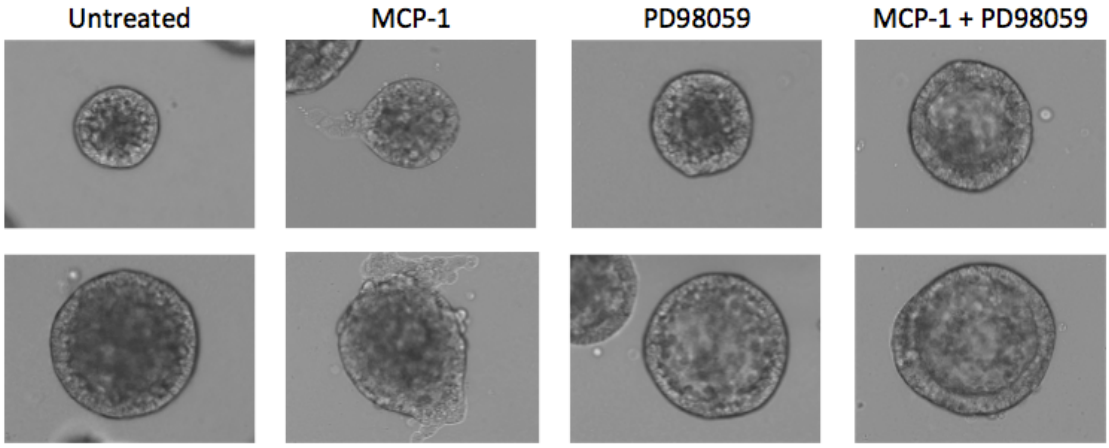

Figure 17: MCP-1 induces invasion of cells away from spheroid and into ECM

MCF10A spheroids treated with MCP-1 produced outgrowth of cells moving away from the spheroids. These cells invaded the Matrigel ECM. In some cases, not pictured here, the cells invaded the matrix to the plastic bottom of the chamber slide and populated the plastic.

In order for the MCF10A cells to invade, they have to break down the ECM surrounding the spheroid (66). This is accomplished by the secretion of matrix metalloproteinases (MMPs), which catalytically break down the components of the ECM. A gelatin zymography assay was employed to test for two commonly upregulated MMPs, 2 and 9. Media from the final 24 hour treatment on the spheroid invasion assay were used to test for secreted MMP-2 and MMP-9. Treatment with MCP-1 did not increase the latent MMP-2 or latent MMP-9 secreted by MCF10A cells, nor did it induce the secretion of the active form of either of these enzymes (Figure 18).

In summary, MCP-1 is inducing invasion of MCF10A cells in 3D through an Erk signaling pathway. MCP-1 treated MCF10A cells are not secreting MMP-2 or MMP-9 to break down the ECM. Therefore, further investigation is required to elucidate which MMPs are activated during MCP-1 induced MCF10A invasion.

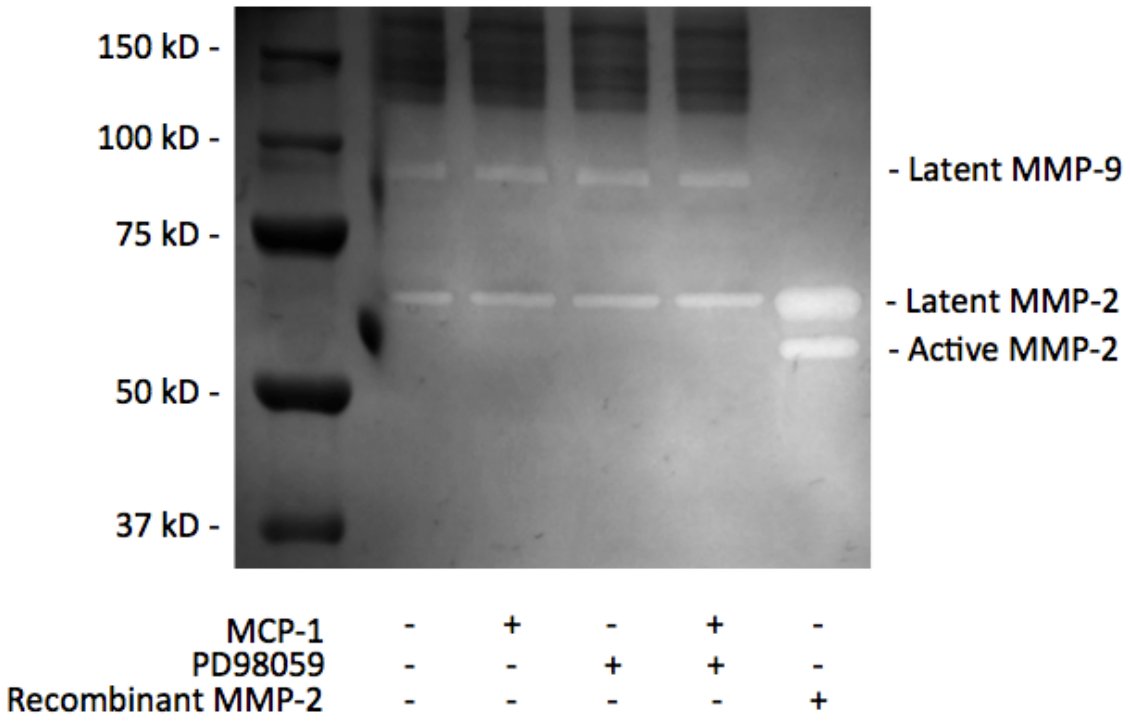

Figure 18: MCP-1 does not induce MMP-2 or MMP-9

Media collected after the last 24 hours of incubation were run on a gelatin zymogram gel. Each medium contained equal amounts of latent or inactive MMP-2 and MMP-9. Recombinant MMP-2 was run as a positive control.

3.5 Direct co-culture of MCF10A cells with ASCs in 3D induces MCF10A cell EMT and invasion

The use of conditioned media or recombinant cytokine treatment does not allow direct paracrine signaling that might occur between two or more cells. Additionally, both paracrine and autocrine feedback loops can form when cells are grown together. Therefore, both MCF10A cells and ASCs were directly co-cultured to determine whether direct co-culture of these cells induced EMT and invasion.

The presence of ASCs induced EMT in a large portion of the MCF10A cells (Figure 19). MCF10A cells lost expression of E-cadherin and upregulated Vimentin. This induction of EMT was not true for all of the cells. There were cells that maintained their epithelial phenotype and expressed E-cadherin.

The size of the ASCs made it possible to distinguish between the mesenchymal MCF10A cells and the mesenchymal ASCs. Adipose stromal cells stain for only Vimentin similarly to the mesenchymal MCF10A cells, but they are larger and elongated.

The MCF10A cells and ASCs were both separated by an ECM gel at the beginning of the experiment. Not only did the mesenchymal MCF10A cells invade down toward the ASCs, but the ASCs invaded toward the MCF10A cells. Confocal microscopy allowed for the visualization of individual planes along the z-axis showing invading cells. Figure 19 shows both MCF10A cells and ASCs in the same plane despite being separated by an ECM gel at the beginning of the experiment (Figure 19). Additionally, after 14 days of co-culture, the ECM was noticeably degraded in the co-

cultured cells compared to the single cell line controls. This degradation occurred in both independent experiments, and it made the immunofluorescence processing difficult. The degradation of the ECM suggests an upregulation of MMPs from the invading cells. Further investigation will be needed to elucidate the mechanism through which the MCF10A cells and ASCs invaded.

Taken together, direct co-culture of MCF10A cells with ASCs in 3D ECM induced EMT in MCF10A cells. Moreover, direct co-culture induced invasion in both the MCF10A cells and ASCs. Future investigations will be necessary to determine whether direct co-culture induced additional cytokine or growth factor secretion, and if any feedback loops were initiated.

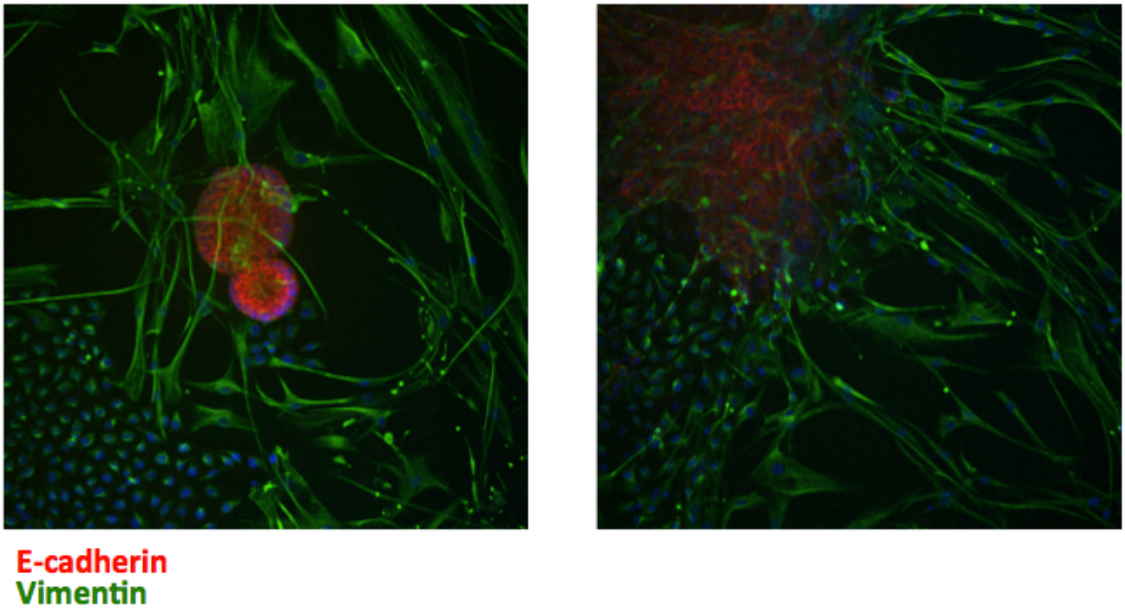

Figure 19: ASCs induce MCF10A EMT and invasion in 3D

MCF10A cells grown in direct co-culture with ASCs for 14 days induced loss of E-cadherin staining and increase in Vimentin staining. Additionally, MCF10A cells invaded down through the Matrigel, and ASCs invaded up through the Matrigel. Mesenchymal MCF10A cells were distinguishable from ASCs by size. ASCs were significantly larger and elongated.

4 Discussion

4.1 Three-dimensional culturing is necessary for MCP-1 induced E-cadherin loss

Monocyte chemoattractant protein-1 is a small inflammatory chemokine that regulates the migration and infiltration of monocytes and macrophages to sites of injury or inflammation (49). MCP-1 binds to CCR2 and can signal through the family of MAP kinases (49,53,57-58). In MCF10A cells, MCP-1 rapidly induced the phosphorylation of Erk1/2. Erk signaling is associated with obesity, involved in EMT, migration, and invasion (61-62, 65, 80-83, 102). Erk signaling is also associated with aggressive TNBC (12). The activation of Erk alone by MCP-1, however, is not sufficient to induce loss of E-cadherin in a non-transformed, mammary epithelial cell line in 2D culture.

MCF10A acini grown in ECM lost E-cadherin expression when treated with MCP-1. The addition of the Erk inhibitor PD98059 inhibited Erk phosphorylation and, consequently, the loss of E-cadherin. PD98059 inhibition of MCP-1 induced E-cadherin loss in 3D suggests that the activation of Erk is necessary for the loss of E-cadherin.

There are examples of cytokine treatments in literature where ECM was necessary to observe a phenotype. In a study of the inflammatoray cytokine IL-6, it was necessary to grow the luminal breast cancer cells in ECM prior to IL6 treatment to induce EMT (27). The synergistic signaling contributed by the ECM, however, has yet to be elucidated in our 3D model of MCP-1 induced E-cadherin loss in non-transformed, mammary epithelial cells.

The extracellular matrix interacts with the basal pole of the MCF10A cells forming acini. The interaction between ECM and cell is mediated through integrins. Integrins are involved in cellular anchorage, and they transmit chemical signals into the cell providing information on its location, local environment, adhesive state, and surrounding matrix. These signals from integrins determine cellular responses such as migration, survival and differentiation. Additionally, integrins provide a context in which the cell responds to other external inputs transmitted by growth factor receptors or G-protein-coupled receptors (68).

Integrins signal through integrin-linked kinase (ILK), which in turn can phosphorylate Akt at S473 and GSK-3β at S9 (69, 70). Akt signaling plays a prominent role in EMT and inhibition of GSK-3β can lead to Snail stabilization and EMT (71-74). Integrin engagement with ECM alone, however, does not induce EMT in MCF10A cells. MCF10A cells are epithelial when they form acini in 3D culture (63). In this study, MCF10A acini stained for E-cadherin and β-catenin localized to the plasma membrane, with little to no Vimentin staining. Additionally, the basal staining of Integrin $\alpha 6$ indicated proper polarity and integrin engagement.

Further investigation into the contribution of ECM and integrin signaling need to be performed in order to elucidate the synergistic signal allowing for the MCP-1 induced E-cadherin loss. Elucidating the role of integrin signaling can be accomplished with the use of pharmacological inhibitors against ILK to determine if integrin signaling contributes to MCP-1 induced E-cadherin loss. Further experiments using individual ECM components, collagen IV or laminin, can be performed to determine which ECM

protein contributes to the MCP-1 induced E-cadherin loss. Elucidating the role of ECM in MCP-1 induced E-cadherin loss provides a potential line of investigation for this project moving forward.

4.2 MCP-1 induces migration in MCF10A cells

MCF10A cells express CCR2, which is the receptor for MCP-1. Thus, it was not surprising when MCP-1 induced migration in MCF10A cells. Regardless, increased migration is still an important phenotype generated by MCP-1. It shows that the cells are responding to MCP-1 treatment. Furthermore, inhibition of migration with PD98059 indicates that migration is controlled through an Erk signaling pathway. While this may be true, cells aren't able to migrate in tissue as they would on plastic. Thus, the more biologically pertinent question was whether they could invade a biological matrix.

4.3 MCP-1 induces invasion in MCF10A cells

In a spheroid gel invasion assay, MCF10A spheroids treated with MCP-1 lost their distinct borders, and cells invaded the surrounding matrix. In some instances, MCF10A cells invaded the matrix and reached the plastic below. This invasion was not observed in the untreated controls. Additionally, PD98059 inhibited MCP-1 from inducing invasion of cells into the surrounding matrix. These data provide evidence of MCP-1 induced invasion in a non-transformed, mammary epithelial cell line. Invasion is more biologically relevant because *in vivo* cells have to pass through basement membranes to escape and metastasize. The primary advantage of the spheroid gel invasion assay is that it mimics *in vivo* invasion where cell clusters with well-established cell-cell interactions break through basement membranes. In a modified Boyden

invasion assay, however, individual cells pass through ECM and a membrane, which does not mimic *in vivo* invasion (17, 66).

Gelatin zymography tested for the presence of MMPs secreted into the media to elucidate the mechanism by which MCF10A cells were invading. Although gelatin zymography can be used to detect several MMPs, it is best for the assessment of the gelatinases: MMP-2 and MMP-9 (75-76). All conditions in the 3D MCF10A spheroid gel invasion assay secreted pro-MMP-2 and pro-MMP-9 into the media. There were no active forms of either MMP-2 or MMP-9 secreted into the media. Thus, neither MMP-2 nor MMP-9 is contributing to the invasion in the MCP-1 treated speroids. There are, however, other MMPs that might be secreted upon treatment with MCP-1.

Collagen gel zymography would be more informative for collagenases, such as MMP-1, 8, and 13 (76). Collagen zymographic gels, however, are not available commercially and can be very difficult to properly polymerize. A Human MMP Antibody Array from RayBiotech is an affective alternative because it will show all of the MMPs secreted into the media. The MCP-1 treated spheroid media could then be compared to all other conditions for changes in MMP secretion. This line of investigation will have to be undertaken by a future investigator within the lab.

4.4 Direct co-culture of MCF10A and ASC cells

Directly co-culturing MCF10A cells with ASCs provides paracrine signaling between the two cell lines that conditioned media alone can not. When both cells are grown together, it is possible that there are feedback loops or additional signaling molecules involved that have yet to be observed. The long-term culture of MCF10A cells

in ASC-conditioned media caused the secretion of IL8 and MCP-1 back into the media. Consequently, there are additional cytokines or growth factors that may be secreted when these cells are grown together.

Though this line of investigation requires further exploration, it is known that by co-culturing both of these cell lines together in 3D produced an EMT where E-cadherin was lost and Vimentin was upregulated. Additionally, the invading cells broke down the ECM to where it was nearly impossible to process the sample for immunofluorescence. Thus, a model system has to be developed where it is possible to study the paracrine signaling of both cell lines and the resulting EMT induced in the MCF10A cells.

This very model system is currently being developed in the Seewaldt lab. Different co-culturing models are being tested to best answer different questions. Once these models are developed, future investigators in the lab will be able to ask questions regarding adipose signaling using several different ASCs to determine if there are differences between ASCs derived from healthy or diseased breasts, obese or non-obese patients, and race.

4.5 The role of MCP-1 and obesity in breast cancer

It is well established that obesity increases the risk of several cancers through its role as a chronic inflammatory condition (14-16). Several groups have shown that there are elevated levels of IL6, IL8, IL1β, TNFα, VEGF, Leptin and MCP-1 in obese adipose and that circulate through the body (13-15, 35-37, 50-51). The constant assault by these inflammatory cytokines, growth factors, and hormones have been shown to contribute

to the development of cancer in several organs. Obesity appears to affect people differently. The Carolina Breast Cancer study showed that obesity in premenopausal women put them at higher risk for TNBC, while postmenopausal women were at increased risk for ER+ cancers (7-9).

Elevated levels of MCP-1, as a result of increased adiposity, can affect the breast two fold. Firstly, there are the direct effects of MCP-1 on the epithelial cells of the breast. This is what was being been studied in this investigation. There are also indirect effects that MCP-1 may have on the formation of a carcinoma of the breast. MCP-1 is a chemokine that regulates the migration and infiltration of monocytes and macrophages (49). Increased adiposity in the breast, and thus, MCP-1, can cause an increase in the number of monocytes and macrophages present in the breast. This increase in monocytes and macrophages could further exacerbate the inflammation in the breast. Furthermore, MCP-1 has been shown to recruit bone marrow derived mesenchymal stem cells to forming tumors (77). Lastly, MCP-1 can induce kidney and peritoneal EMT and fibrosis (78-79, 90-94). Taken together, MCP-1 contributes to carcinogenesis, but further investigation will be required to elucidate the full extent to which MCP-1 is involved in mammary carcinogenesis.

This investigation has provided data that suggest that MCP-1, an adipose derived chemokine, can induce the loss of E-cadherin and invasion in a non-transformed, mammary epithelial cell line. The loss of E-cadherin is a key step in EMT, and invasion is a necessary step in the metastatic process (20). Both EMT and distal metastasis associate with aggressive triple negative breast cancers (11-12, 24-25, 61-62,

85, 98). Although not an exhaustive investigation, this study provides a foundation from which future investigators can begin to ask questions regarding MCP-1 and other adipose-derived cytokine signaling in early mammary carcinogenesis.

Works Cited

1. "Cancer Among Women." *Centers for Disease Control and Prevention*. Centers for Disease Control and Prevention, 02 Jan. 2013. Web. 27 July 2013.

2. Noone AM. et. al. (eds). *SEER Cancer Statistics Review, 1975–2009 (Vintage 2009 Populations),* National Cancer Institute. 2012.

3. Howlader N, et al., eds. *SEER Cancer Statistics Review, 1975-2008*. Bethesda, MD: National Cancer Institute; 2011.

4. Glux, O., C. Liedtke, N. Gottschalk, L. Pusztai, U. Nitz, and N. Harbeck. "Triple-negative Breast Cancer - Current Status and Future Directions." *Annals of Oncology* 20.10 (2009): 1913-927.

5. Bauer, K. R., Brown, M., Cress, R. D., Parise, C. A. and Caggiano, V. (2007), Descriptive analysis of estrogen receptor (ER)-negative, progesterone receptor (PR)-negative, and HER2-negative invasive breast cancer, the so-called triple-negative phenotype. Cancer, 109: 1721–1728.

6. Perou, Charles M. & The Cancer Genome Atlas Network "Comprehensive Molecular Portraits of Human Breast Tumours." *Nature* 490 (2012): 61-70.

7. Carey, Lisa A. et al. "Race, Breast Cancer Subtypes, and Survival in the Carolina Breast Cancer Study." *JAMA* 295 (2006): 2492 – 2502.

8. Moorman, Patricia G. et al. "Race, Antropometric Factors, and State at Diagnosis of Breast Cancer." *AJE* 153, 3 (2001): 284-291.

9. Millikan, Robert C. et al "Epidemiology of basal-like breast cancer." *Breast Cancer Res Treat* 109 (2008): 123-139.

10. Newman, Beth. et al "Frequency of Breast Cancer Attributable to BRCA1 in a Population-Based Series of American Women." *JAMA* 279 (1998): 915 – 921.

11. Lehmann, Brian D. et al "Identification of human triple-negative breast cancer subtypes and preclinical models for selection of targeted therapies." *JCI* 121 (2011): 2750 – 2767.

12. Bartholomeusz, C. et al "High ERK protein expression levels correlate with shorter survival in triple-negative patients." *Oncologist* 17 (2012): 766-774.

13. Rondinone, Crista M. "Adipocyte-Derived Hormones, Cytokines, and Mediators." *Endocrine* 29 (2006): 81-90

14. Lithgow, Diana. et al "Chronic Inflammation and Breast Pathology: A Theoretical Model." *Biological Research for Nursing* 7 (2005): 118-129

15. Das, U. N. "Is Obesity an Inflammatory Condition?" *Nutrition* 17 (2001): 953-966

16. Pilie, Patrick G. et al "Protein Microarrary Analysis of Mammary Epithelial Cells from Obese and Nonobese Women at High Risk for Breast Cancer: Feasibility Data." *Cancer Epidemiology, Biomarkers & Prevention* 20 (2011): 476-482

17. Kramer, Nina. et al. "*In vitro* cell migration and invasion assays." *Mutation Research* 752 (2013): 10-24

18. Howlett, M. et al "Cytokine signaling via gp130 in gastric cancer." *BBA* 1793 (2009): 1623-1633.

19. Hartman, Zachary C. et al "Growth of triple-negative breast cancer cells relies upon coordinate autocrine expression of the pro-inflammatory cytokines IL-6 and IL-8." *Cancer Res* 73 (2013) 3470-3480

20. Kalluri, Raghu and Weinberg, Robert A. "The basics of epithelial-mesenchymal transitions." *JCI* 119 (2009): 1420-1428

21. Thomson, Stuart. et al "A systems view of epithelial-mesenchymal transition signaling states." *Clin Exp Metastasis* 28 (2011): 137-155

22. Micalizzi, Douglas S. et al "Epithelial-Mesenchymal Transition in Cancer: Paralles Between Normal Development and Tumor Progression." *J Mammary Gland Biol Neoplasia* 15 (2010): 117-134

23. Garcia de Herreros, Antonio. et al "Cooperation, amplification, and feed-back in epithelial-mesenchymal transition." *BBA* 1825 (2012) 223-228

24. Sarrio, David. et al "Epithelial-Mesenchymal Transition in Breast Cancer Relates to the Basal-like Phenotype." *Cancer Research* 68 (2008): 989-997

25. Blick, T. et al "Epithelial mesenchymal transition traits in human breast cancer cell lines." 25 (2008): 629-642

26. Chua, HL. et al "NF-kB represses E-cadherin expression and enhances epithelial to mesenchymal transition of mammary epithelial cells: potential involvement of ZEB1 and ZEB-2." *Oncogene* 26 (2007): 711 – 724

27. Sullivan, NJ. et al "Interleukin-6 induces an epithelial-mesenchymal transition phenotype in human breast cancer cells." *Oncogene* 28 (2008): 2940-2947

28. Sehgal, Pravin B. “Interleukin-6 induces increased motility, cell-cell and cell-substrate dyshesion and epithelial to mesenchymal transformation (EMT) in breast cancer cells.” *Oncogene* 29 (2010): 2599-2603

29. Schneider, David. et al “Dynamics of TGF-beta induced epithelial-to-mesenchymal transition monitored by Electric Cell-Substrate Impedance Sensing.” *BBA* 1813 (2011) 2099-2107

30. Fernando, R I. et al “IL-8 signaling plays a critical role in the epithelial-mesenchymal transition of human carcinoma cells.” *Cancer Research* 15 (2011): 5296-5306

31. Turner, NC. et al. “Basal-like breast cancer and the BRCA1 pheonotype.” *Oncogene* 25 (2009): 5846-5853

32. Zavadil, Jiri. et al “TGF-beta and epithelial-mesenchymal transitions.” *Oncogene* 24 (2005): 5764-5774

33. Maeda, Masato. et al “Cadherin switching: essential for behavioral but not morphological changes during an epithelium-to-mesenchyme transition.” *J Cell Science* 118 (2005): 873-887

34. Brooksby, Ben. et al “Imaging breast adipose and fibroglandular tissue molecular signatures by using hybrid MRI-guided near-infrared spectral tomography.” *PNAS* 103 (2006): 8828-8833

35. Place, Andre E. et al “The microenvironment in breast cancer progression: biology and implications for treatment.” *Breast Cancer Research* 13 (2011): 227-238

36. Creydt, Virginia P. et al “Human adipose tissue from normal and tumoral breast regulates the behavior of mammary epithelial cells.” *Clinical andTranslational Oncology* 15 (2012): 124-131

37. Walter, M. et al “Interleukin 6 secreted from adipose stromal cells promote migration and invasion of breast cancer cells.” *Oncogene* 30 (2009): 2745-2755

38. Nieman, Kristin M. et al “Adipocytes promote ovarian cancer metastasis and provide energy for rapid tumor growth.” *Nature Medicine* 17 (2011): 1498-1504

39. Kilroy, Gail E. et al “Cytokine profile of human adipose-derived stem cells: expression of angiogenic, hematopoietic, and pro-inflammatory factors.” *J Cellular Physiology* 212 (2007): 702-709

40. Ribeiro, Ricardo. et al "Human periprostatic adipose tissue promotes prostate cancer aggressiveness *in vitro*." *Journal of Experimental & Clinical Cancer Research* 31 (2012)

41. Pavlovich, Amira L. et al "Adipose stroma induces branching morphogenesis of engineered epithelial tubules." *Tissue Engineering* 16 (2010): 3719-3726

42. Chandler, Emily M. et al "Implanted adipose progenitor cells as physicochemical regulators of breast cancer." *PNAS* (2012)

43. Adams, A. M. et al "Use of adipose-derived stem cells to fabricate scaffoldless tissue-engineered neural conduits *in vitro*." *Neuroscience* 201 (2012): 349-356

44. Wang, Xiuli. et al "Preadipocytes stimulate ductal morphogenesis and functional differentiation of human mammary epithelial cells on 3D silk scaffolds." *Tissue Engineering* 15 (2009) 3087-3098

45. Choy, L. et al "Transforming growth factor-beta inhibits adipocyte differentiation by Smad3 interacting with CCAAT/enhancer binding protein (C/EBP) and repressing C/EBP transactivation function." *JBC* 11 (2003): 9609-9619

46. Liotta LA. et al. "Metastasis suppressor genes.". *Important Adv. Oncol.* (1991): 85–100.

47. Carr, M. W. er al. "Monocyte chemoattractant protein 1 acts as a T-lymphocyte chemoattractant". *Proceedings of the National Academy of Sciences of the United States of America* 91 (1994): 3652–3656.

48. Soule, Herbert D. et al "Isolation and Characterization of a spontaneously immortalized human breast epithelial cell line, MCF-10." *Cancer Research* 50 (1990): 6075-6086

49. Deshmaine, Satish L. et al "Monocyte chemoattractant protein-1 (MCP-1): an overview." *Journal of Interferon & Cytokine Research* 29 (2009): 313-326

50. Westerbacka, J. et al. "Insulin regulation of MCP-1 in human adipose tissue of obese and lean women." *Am J Physiol Endocrinol Metab* 5 (2008): 841-845

51. Kamei, N. et al "Overexpression of monocyte chemoattractant protein-1 in adipose tissues causes macrophage recruitment and insulin resistance." *JBC* 36 (2006): 26602-26614

52. Kaurihara, Takao. et al. "Defects in macrophage recruitment and host defense in mice lacking the CCR2 chemokine receptor." *J. exp. Med.* 186 (1997): 1757-1762

53. Schecter, Alison D. et al. "MCP-1-dependent signaling in CCR2-/- aortic smooth muscle cells." *J. Leukocyte Biol.* 75 (2004): 1079-1085

54. Zhang, T. et al "Migration of cytotoxic T lymphocytes toward melanoma cells in three-dimensional oranotypic culture is dependent on CCL2 and CCR4." *Eur J Immunol* 2 (2006) 457-467

55. Craig, M. J. et al. "CCL2 (monocyte chemoattractant protein-1) in cancer bone metastases." *Cancer and Metastasis Review* 25 (2006): 611-619

56. Ogilvie, Patricia. et al. "Unusual chemokine receptor antagonism involving a mitogen-activated protein kinase pathway. *Journal of immunology* 127 (2004): 6715-6722

57. Ashida, Noboru. et al. "Distinct signaling pathways for MCP-1-dependent integrin activation and chemotaxis." *JBC* 276 (2001): 16555-16560

58. Fang, Wei Bin. et al. "CCL2/CCR2 chemokine signaling coordinates survival and motility of breast cancer cells through smad3 protein – and p42/44 mitogen-activated protein kinase (MAPK) – dependent mechanisms." *JBC* 287 (2012): 36593-36608

59. D'Amato NC. et al. "Evidence for Phenotypic Plasticity in Aggressive Triple-Negative Breast Cancer: Human Biology is Recapitulated by a Novel Model System." *Plos One* 7 (2012) e45684

60. Bhat-Nakshatri, Poornima. et al. "SLUG/SNAI2 and Tumor Necrosis Factor Generate Breast Cells with CD44+/CD24- Phenotype." *BMC Cancer* 10 (2010) 411

61. Sejeong, Shin. et al. "Erk2 but not Erk1 induces epithelial-to-mesenchymal transformation via DEF motif-dependent signaling events." *Molecular Cell* 38 (2010):114-127

62. Santamaria, Patricia G. et al. "Deconstructing Erk signaling in tumorigenesis." *Molecular Cell* 38 (2010): 3-5

63. Debnath, Jayanta. et al. "Morphogenesis and oncogenesis of MCF-10A mammary epithelial acini grown in three-dimentional basement membrane cultures." *Methods* 30 (2003): 256-268

64. Gilles, Christine. et al. "Vimentin contributes to human epithelial cell migration." *Journal of Cell Science* 112 (1999): 4615-4625

65. Huang, Cai. et al. "MAP kinases and cell migration." *Journal of Cell Science* 117 (2004) 4619-4628

66. Valster, Aline. et al. "Cell migration and invasion assays." *Methods* 37 (2005): 208-215

67. Carter, Jennifer C. et al. "Mature breast adipocytes promote breast cancer cell motility." *Experimental and Molecular Pathology* 92 (2012): 312-317

68. Harburger, David S. et al. "Integrin signaling at a glance." *Journal of Cell Science* 122 (2009): 159-163

69. Persad, S. et al. "Regulation of protein kinaseB/Akt-serine 473 phosphorylation by integrin-linked kinase: critical roles for kinase activity and amino acids arginine 211 and serine 343." *JBC* 276 (2001): 27462-27469

70. Persad, S. et al "Tumor suppressor PTEN inhibits nuclear accumulation of beta-catenin and T cell/lymphoid enhancer factor 1-mediated transcriptional activation." *JBC* 153 (2000): 1161-1174

71. Bellacosa, A. et al. "PI3K/AKT pathway and the epithelial-mesenchymal transition." *Cancer Genome and Tumor Microenvironment* Chapter 2 (2010): 11-27

72. Grill, SJ. et al. "The protein kinase Akt induces epithelial mesenchymal transition and promotes enhanced motility and invasiveness of squamous cell carcinoma lines." *Cancer Research* 63 (2003): 2172-2178

73. Larue, Lionel. et al. "Epithelial-mesenchymal transition in development and cancer: role of phosphatidylinositol 3' kinase/AKT pathways." *Oncogene* 24 (2005): 7443-7454

74. Doble, BW. et al. "Role of glycogen synthase kinase-3 in cell fate and epithelial-mesenchymal transitions." *Cell Tissues Organs* 185 (2007) 73-84

75. Toth, Marta. et al. "Assessment of gelatinases (MMP-2 and MMP-9) by gelatin zymography." *Metastasis Research Protocols* in Methods in Molecular Medicine 57 (2001): 163-174

76. Snoek-van Deurden, Patricia A.M. et al. "Zymographic techniques for the ananlysis of matrix metalloproteinases and their inhibitors." *BioTechniques* 38 (2005): 73-83

77. Dwyer, R.M. et al. "Monocytes chemotactic protein-1 secreted by primary breast tumors stimulates migration of mesenchymal stem cells." *Clin Cancer Res* 13 (2007): 5020-5027

78. Yanez-Mo, Maria. et al. "Peritoneal dialysis and epithelial-to-mesenchymal transition of meseothelial cells." *NEJM* 348 (2003): 403-413

79. Lee, Sun Ha. et al. "The monocyte chemoattractant protein-1 (MCP-1)/CCR2 system is involved in peritoneal dialysis-related epithelial-mesenchymal transition of peritoneal mesothelial cells." *Laboratory Investigation* 92 (2012): 1698-1711

80. Lo, Chi-Wen. et al. "IL-6 trans-signaling in formation and progression of malignant ascites in ovarian cancer." *Cancer Research* 71 (2010): 424

81. Yang, Ronghua. et al. "Leptin Signaling and Obesity: Cardiovascular Consequences." *Circulation Research* 101 (2007): 545-559

82. Knall, C. et al. "Interleukin-8 regulation of the Ras/Raf/mitogen activated protein kinase pathway in human neutrophils." *J. Biol. Chem.* 271 (1996): 2832-2838

83. Vallavicencio, A. et al. "The effect of overweight and obesity on proliferation and activation of AKT and ERK in human endometria." *Gynecological Oncology* 117 (2010): 96-102

84. Atchly, DP. et al. "Clinical and pathological characteristics of patients with BRCA-positive and BRCA-negative breast cancer." *J Clin Oncol* 26 (2008): 4282-4288

85. Voduc, KD. et al. "Breast cancer subtypes and the risk of local and regional relapse." *J Clin Oncology* 28 (2010): 1684-1691

86. Stead, LA. et al. "Triple-negative breast cancers are increased in black women regardless of age or body mass index." *Breast Cancer Res* 11 (2009): R18

87. Tzanavari, T. et al. "TNF-alpha and obesity." *Curr Dir Autoimmun* 11 (2010): 145-156

88. Gilbert, CA. et al. "Cytokines, obesity, and cancer: new insights on mechanisms linking obesity to progression." *Annu Rev Med* 64 (2013): 45-57

89. Yan, D. et al. "Leptin-induced epithelial-mesenchymal transition in breast cancer cells required activation via Akt/GSK3- and MTA1/Wnt1 protein-dependent pathways." *J Biol Chem* 287 (2012): 8598-8612

90. Munshi, R. et al. "MCP-1 gene activation marks acute kidney injury." *J Am Soc Nephrol.* 22 (2011): 165-175

91. Viedt, Christiane. et al. "Monocyte chemoattractant protein-1 (MCP-1) in the kidney: does it more than simply attract monocytes?" *Nephrol. Dial. Transplant.* 17 (2002): 2043-2047

92. Wada, Takashi. et al. "Gene therapy via blockade of monocyte chemoattractant protein-1 for renal fibrosis." *J Am Soc Nephrol* 15 (2004): 940-948

93. Kitagawa, K. et al. "Blockade of CCR2 ameliorates progressive fibrosis in kidney." *Am J Pathology* 165 (2004): 237-246

94. Li HL. et al. Effects of induction of tubular epithelial-myofibroblast transition by monocyte chemoattactant protein-1 and mechanism thereof: an in vitro experiment." *ZYXZZ* 88 (2008): 400-405

95. Bauer, KR. et al. "Descriptive analysis of estrogen receptor (ER)-negative, progesterone receptor (PR)-negative, and HER2-negative invasive breast cancer, the so called triple-negative phenotype – a population-based study from the California Cancer Registry." *Cancer* 109 (2007): 1721-1728

96. Liedtke C, Hess KR, Karn T et al. "The prognostic impact of age in patients with triple-negative breast cancer." *Breast Cancer Research and Treatment*. 138 (2013): 591-599

97. Stead LA, Lash TL, Sobieraj JE, et al. "Triple-negative breast cancers are increased in black women regardless of age or body mass index." *Breast Cancer Res.* 11(2009): R18

98. Ihemelandu CU, Leffall LD Jr, Dewitty RL, et al. "Molecular breast cancer subtypes in premenopausal African-American women, tumor biologic factors and clinical outcome." *Ann Surg Oncol*. 14(2007): 2994-3003

99. Lund MJ, Trivers KF, Porter PL, et al. "Race and triple negative threats to breast cancer survival: a population-based study in Atlanta, GA." *Breast Cancer Res Treat.* 113 (2009): 357-370

100. Morris, GJ. et al. "Differences in breast carcinoma characteristics in newly diagnosed African-American and Caucasian patients – a single-institution compilation compared with the National Cancer Institute's Surveillance, Epidemiology, and End Results database." *Cancer* 110 (2007): 876-884

101. Pierobon, M. et al. "Obesity as a risk factor for triple-negative breast cancers: a systematic review and meta-analysis." *Breast Cancer Res Treat* 137 (2013): 307-314

102. Von Thun, Anne. et al. "Erk2 drives tumour cells migration in 3D microenvironments by suppressing expression of Rab17 and Liprin-β2." *JCS* 125 (2012): 1465-1477